

LAL-Orsay Seminar, 02/19/2010

From Tracks to Electrons

Thomas Koffas
(CERN)

Overview

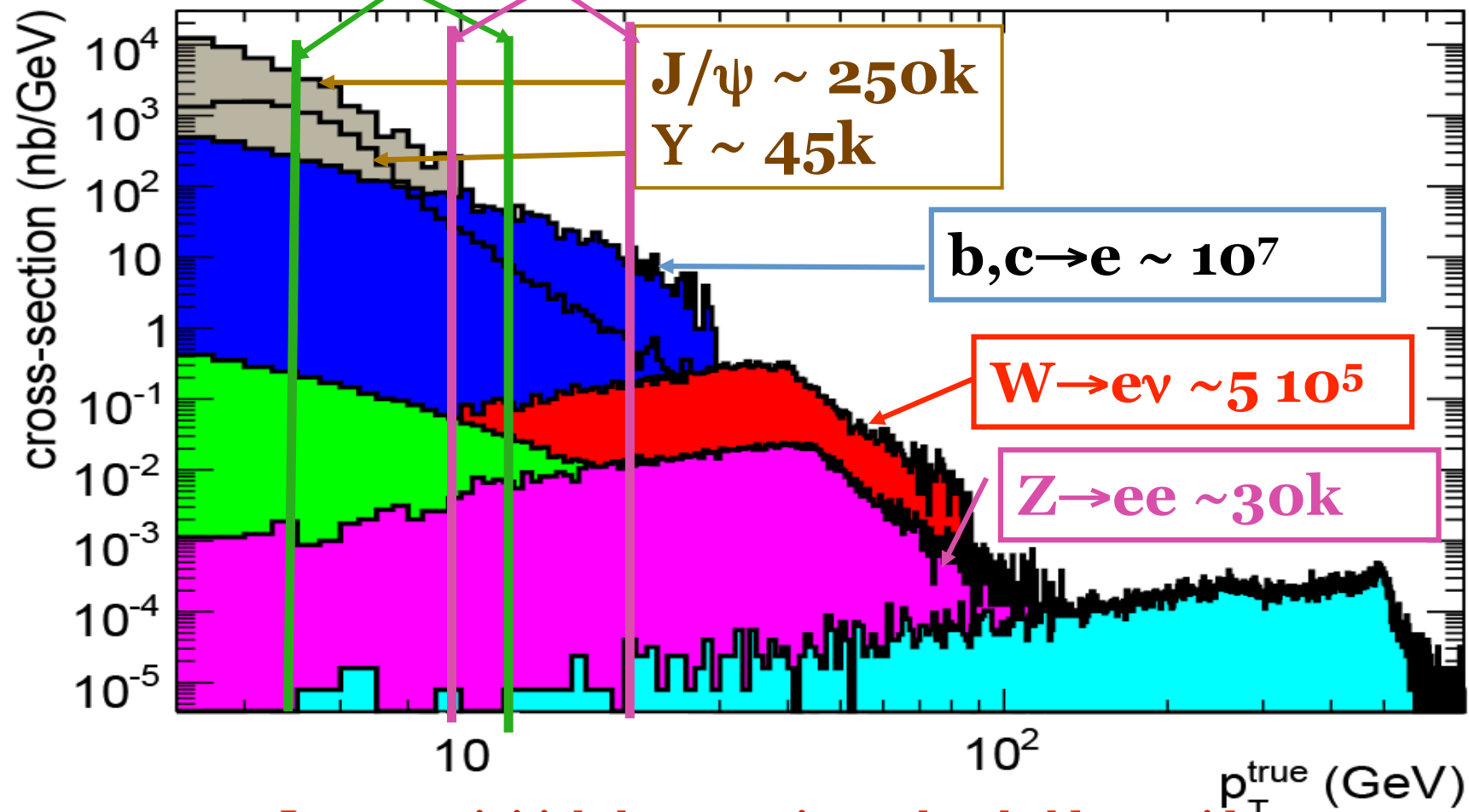
- Electrons in ATLAS
- Track Reconstruction in ATLAS
 - Si-Seeded Tracking
 - TRT-Seeded Tracking (back-tracking)
 - Stand-alone TRT tracks
 - Track Fitting
 - Tracking Performance
- Tracking for Electrons
 - Inner Detector based Electron identification
 - Bremsstrahlung Corrections
- Electrons from Converted Photons
 - Conversion Reconstruction in the Tracker
 - Vertex refitting
- Electron/Converted Photon Reconstruction in e/ γ
 - Track/Vertex Matching to Electromagnetic Clusters
 - Electron 4-Momentum estimation
 - Converted Photon Recovery
 - Electron/Photon Reconstruction Performance
- Tracker Material Estimation with Photon Conversions
- Conclusions

Electrons in ATLAS with Early Data

Threshold for ee

Threshold for single e

$L=10^{31} \text{ cm}^{-2} \text{ s}^{-1}, 100 \text{ pb}^{-1}$



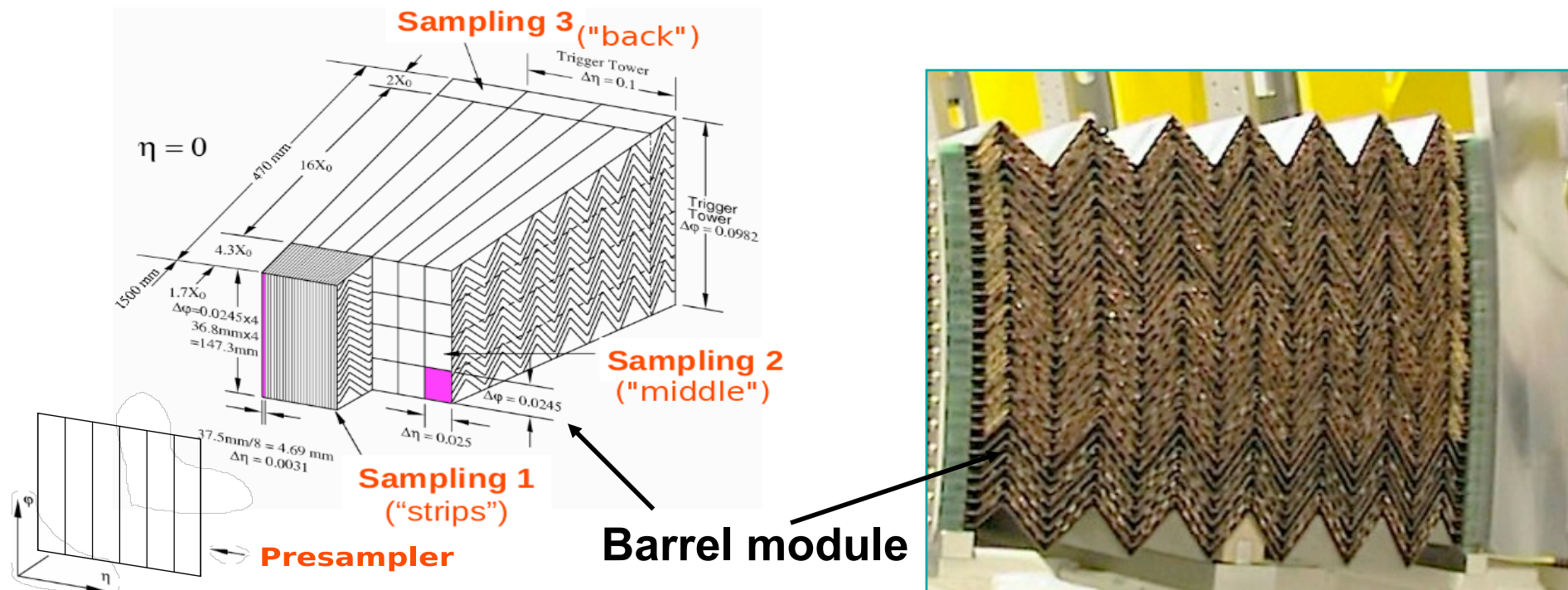
Lower- p_T initial electron trigger thresholds provide

ten times larger statistics for pairs (J/ψ) and inclusive (b/c to e)

Loose photon trigger at 20 GeV E_T threshold will provide $\sim 10^7$ isolated γ per 100 pb^{-1}
(but only ~ 10000 photons with $E_T > 100$ GeV, important for jet calibration)

Crucial for early understanding of detector and trigger

LAr EM Calorimeter description



EM Calo (Presampler + 3 layers):

- Presampler $0.025 \times 0.1 (\ x\phi)$
⇒ Energy lost in upstream material
- Strips $0.003 \times 0.1 (\ x\phi)$
⇒ optimal separation of showers in non-bending plane, pointing
- Middle $0.025 \times 0.025 (\ x\phi)$
⇒ Cluster seeds
- Back $0.05 \times 0.025 (\ \eta \times \phi)$
⇒ Longitudinal leakage

- LAr-Pb sampling calorimeter (barrel)
- Accordion shaped electrodes
- Fine longitudinal and transverse segmentation
- EM showers (for e^+ and photons) are reconstructed using calorimeter cell-clustering
- Total coverage $|\eta| < 3.2$ (precision < 2.5)

The ATLAS Tracker

The Inner Detector (ID) is organized into three sub-systems:

Pixels

- 1 removable barrel layer
- 2 barrel layers
- 4 end-cap disks on each side ($0.8 \cdot 10^8$ channels)

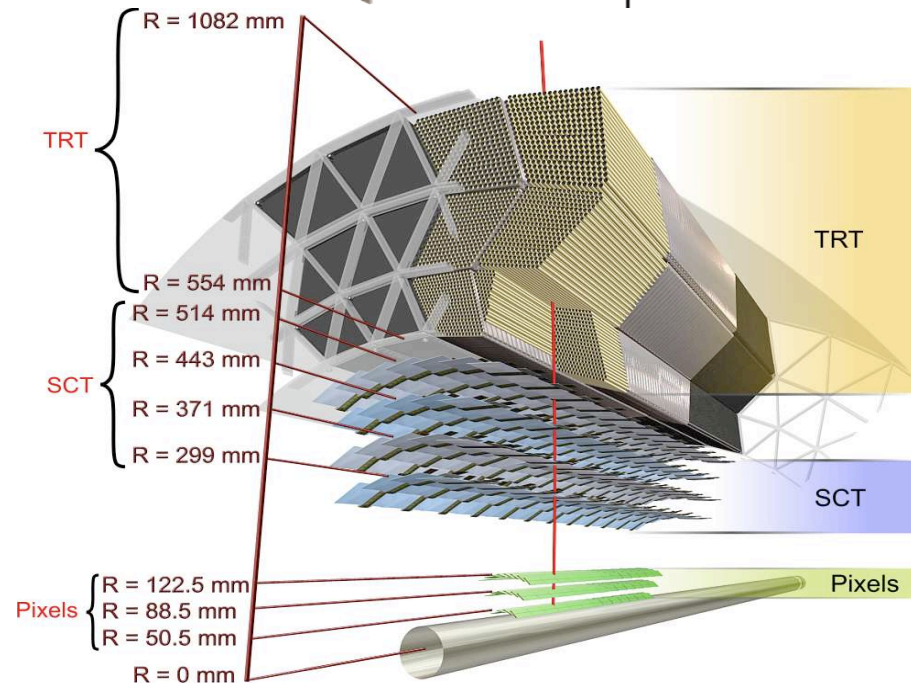
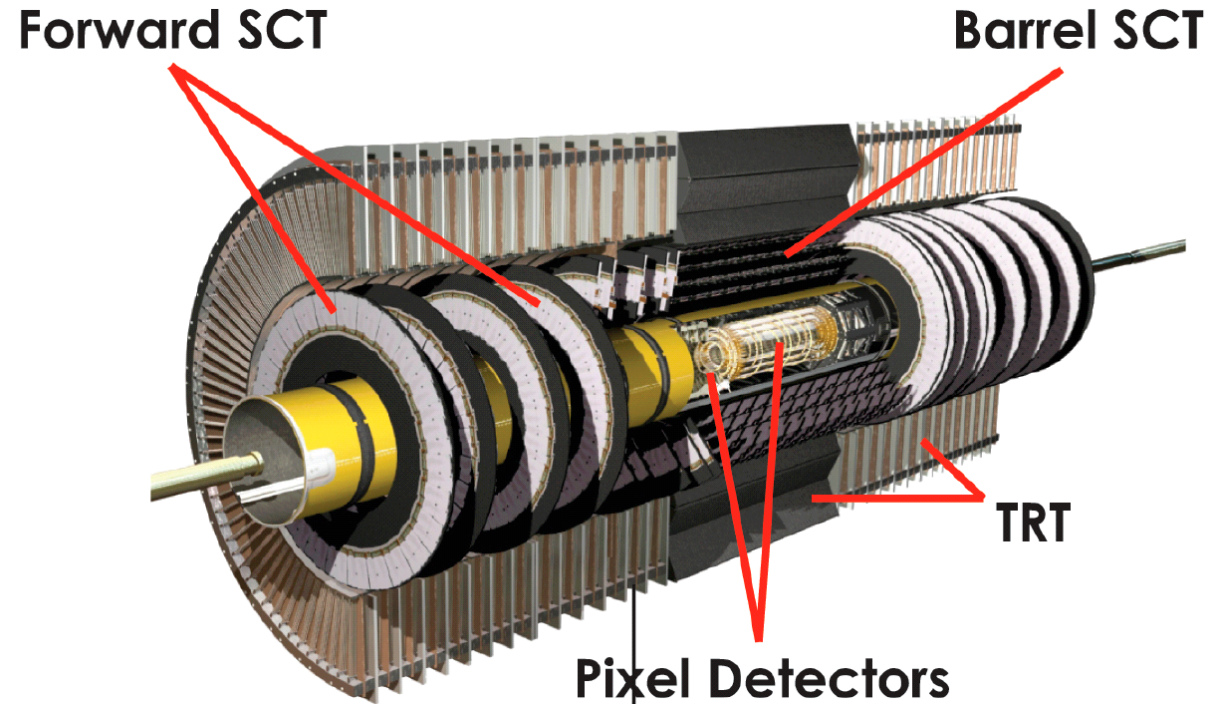
Silicon Tracker (SCT)

- 4 barrel layers
- 9 end-cap wheels on each side ($6 \cdot 10^6$ channels)

Transition Radiation Tracker (TRT)

- Axial barrel straws
- Radial end-cap straws
- ~36 straws per track ($4 \cdot 10^5$ channels)
- electron PID capability

Total coverage $|\eta| < 2.5$



Overview of the ATLAS Track Reconstruction

- The combination of precision trackers at small radii with the TRT at a larger radius allows for a robust pattern recognition and high precision measurements at both the R- ϕ and R-z planes
- Charged particles with $p_T > 0.5$ GeV and $|\eta| < 2.5$ are reconstructed
- A three-step reconstruction sequence is in place:
 - Inside-out tracking seeded by precision hits and developing outwards towards the larger radii
 - Efficient reconstruction of charged particles originating at the primary vertex
 - Precision hits ensure high efficiency in reconstructing tracks in dense environments, e.g. jets
 - Outside-in tracking seeded by TRT straw hits and moving inwards towards the precision layers
 - Efficient reconstruction of charged particles from long lived particle decays (V0s, conversions)
 - Second-pass sequence for improving the efficiency of the inside-out tracking
 - Stand-alone TRT tracking for charged particles created at larger radii in the tracker
 - Reconstruct all charged particle tracks that do not have Si hits assigned to them
 - Common seeding with the outside-in track reconstruction
- A dedicated low- p_T tracking is in place for charged particles with $p_T > 100$ MeV
 - Pattern recognition within the pixel and Si-strip detectors, no TRT counterpart
- The above algorithms are applied sequentially in the order listed here
- All tracks reconstructed by the algorithms described above are stored in one container
 - Common event model (EDM) allows for that
 - Author label can provide the method used for reconstructing the track in question

Inside-out Track Reconstruction: Si Seeds

- The first step is the creation of Space Points
 - 3D representations of the Si detector measurements
 - In the case of pixel this is a one-to-one map of clusters to space points
 - Pixel modules provide a 2D local measurement
 - In the case of the Si strips two clusters are needed on either side of a layer
 - Two Si modules are glued back-to-back to form a layer
 - They are rotated with a stereo angle with respect to each other
 - Together with a beam spot constraint they can be used to reconstruct a space point
- The second step is the reconstruction of a track seed using the space points
 - Space points are initially ordered according to their ϕ, z, R coordinates
 - A pattern of three space points is formed irrespective of whether they are pixel or Si-strip ones
 - Possible patterns can therefore be (p,p,p), (p,p,s), (p,s,s), (s,s,s)
 - All three space points are required to be on a line on the (R,z) plane
 - A linear extrapolation to the origin (0,0,0) is performed and a maximum z-impact is required
 - The curvature is then computed in the (R, ϕ) plane and a minimum p_T is imposed
 - Finally a maximum impact parameter with respect to (0,0,0) is required
 - A modification of the above is used in the case of Heavy Ion collisions
 - Fast primary vertex reconstruction using the seeds is performed
 - A tolerance region for the predicted vertices can be used as a selection cut
 - It has been shown that the (p,p,p) and (s,s,s) seed patterns result in reduced fakes

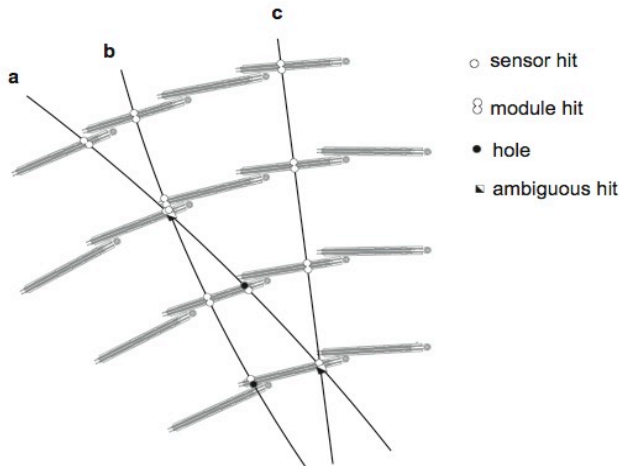
Inside-out Track Reconstruction: Pattern Recognition

- After the three space-point seed formation the pattern recognition proper commences
- Each seed provides enough directional information to build an element road
 - Indicates which Si detector elements should be intercepted by the particle trajectory
- Only clusters from these detector elements will be further considered
- A Kalman fitter-smoother procedure is used within the seed clusters
 - Additional clusters in-between the original space-point clusters may be collected
- Extensions are then searched for from both ends of the seed
 - A Kalman fitter-smoother procedure is again used to simultaneously follow the trajectory and include successive hits in the track candidate
 - It progressively updates the track information, predicting precisely the track representation on the next measurement surface
 - Since detector elements contain more than one cluster this results in the most likely extension of the particle trajectory
 - Outliers are detected immediately due to their large contribution to the χ^2 of the track candidate
- Not all space-point seeds lead to track candidates
 - Normally only in ~10% of the cases the seed is extended to a track candidate
- It is also possible to produce more than one track candidate from a single space-point seed
 - Very rare in the case of the ATLAS Si tracker.

Inside-out Track Reconstruction: Ambiguity Solving

- The resultant number of track candidates is still rather high
 - Many of the candidates share hits, are incomplete, or describe fake tracks
- Appropriate to rank the track candidates according to their likelihood to belong to real particles
- Different track characteristics are used to form a track score
 - Some can be beneficial, others will result to a penalty
 - Measurements of different sub-detectors are weighted, pixel clusters being ranked higher

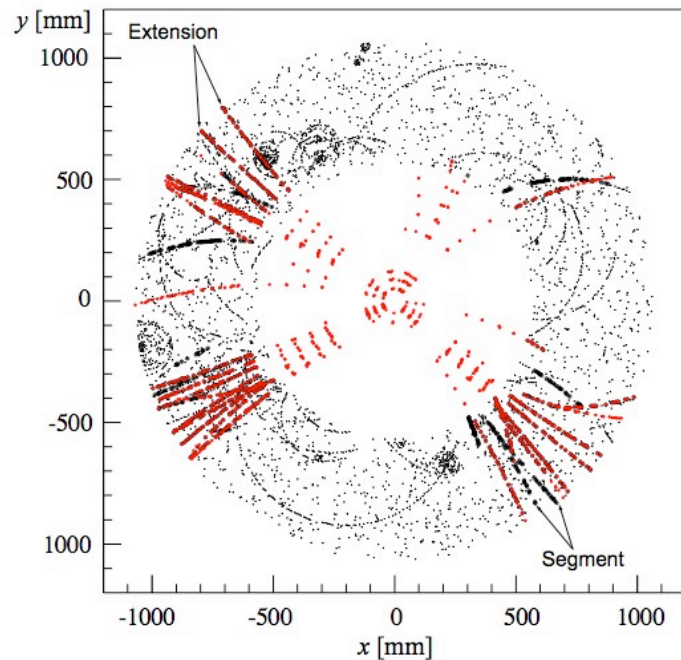
Track Characteristics	Detector	Effect on track score
B-layer hole	Pixel	Strong penalty
Layer hole	Pixel	Penalty
Overlap hit	Pixel, SCT	Strong benefit
Sensor hole	SCT	Weak penalty
Layer hole	SCT	Strong penalty



- Shared hits are assigned to the track with highest score
- Tracks are refitted, scored again and re-ordered
- Iterative procedure:
 - Tracks with highest scores are stored
 - Tracks below a certain quality level are abandoned

Inside-out Track Reconstruction: TRT Extension

- Ambiguity resolved Si tracks need to be extended towards the TRT
 - Si track should not be modified, TRT hits are added to the existing Si hits
- Using the estimated Si track parameters a road is built inside the TRT
- TRT hit coordinates (expressed in R- ϕ for barrel or R-z for the endcaps region) are used
- A line fit is then performed to determine whether the TRT hit is compatible with the Si track

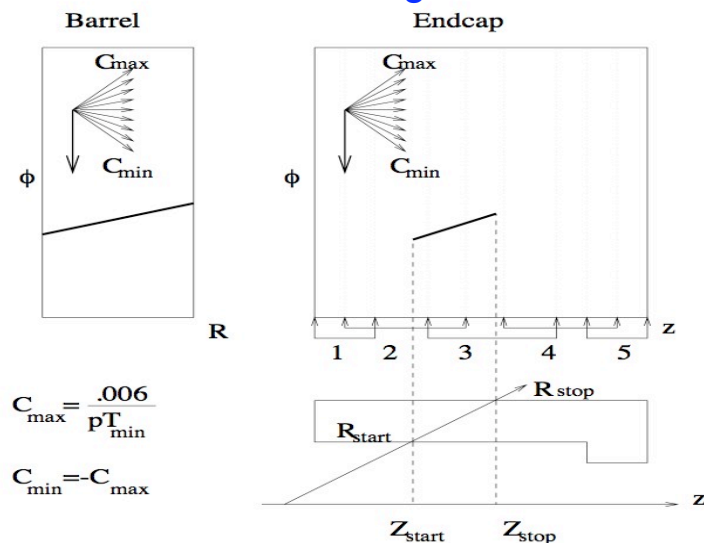


- A map of Si-tracks and possible extensions is produced
- The extended track is evaluated against the pure Si track
 - The extended track is fitted
 - Si hits could be flagged as outliers during the fit
 - The fit quality is compared against that of the Si track
 - The extension is kept if the quality is better
 - The TRT-extension hits are flagged as outliers if not

The main reason for failing to assign a TRT extension to Si tracks is strong energy losses, primarily of electrons, due to interactions with the tracker material

Outside-in Track Reconstruction: TRT Segment Finding

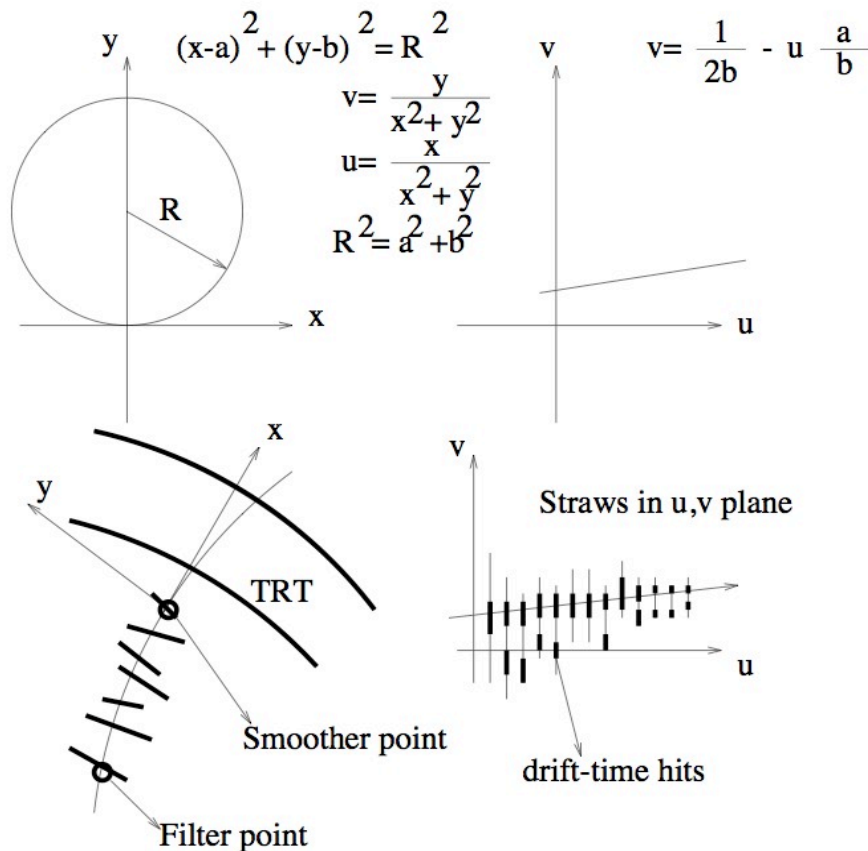
- 2-step procedure, global pattern search and local pattern recognition with track-segment building
- No information along the straw direction in TRT measurements
 - Global pattern recognition needs to be done in appropriate projected planes
 - R- ϕ plane in the TRT barrel
 - z- ϕ plane in the TRT endcap
- Assume that tracks originate roughly at the primary vertex region with $p_T > 500$ MeV
 - Track projections almost straight lines in R- ϕ and rigorous straight lines in z- ϕ planes
 - The track trajectory slope provides measurement of p_T in R- ϕ and p_z in z- ϕ planes
- Use the Hough transformation to extract straight line patterns from an image
 - In R- ϕ and z- ϕ planes with fixed granularity, same number of straight line patterns exist
 - Transform into the parameter space of a straight line using two variables:
 - (ϕ_0, c_T) for barrel, with ϕ_0 the initial azimuthal angle, c_T the inverse momentum parameter
 - (ϕ_0, c_z) for endcap, with ϕ_0 the initial azimuthal angle, c_z the inverse momentum parameter
 - Plot these variables in a two-dimensional parameter plane
 - Straw hits lying on the same line will fall in one (ϕ_0, c) cell
 - Global track segment search reduces to finding local maxima in a two-dimensional histogram



- Define straight lines (roads) for each ϕ_0 and curvature c
- Start/stop is $R_{start}(z_{start})$, $R_{stop}(z_{stop})$ for barrel/endcaps
- Use η slices to reduce number of overlaying tracks
- Calculate hit straw boundaries for a given curvature c
- Order in ascending values of ϕ_0
- Estimate number of crossed straws, compare to max number
- Time needed proportional to $N \log(N)$, N number of straw hits

Outside-in Track Reconstruction: TRT Segment Finding

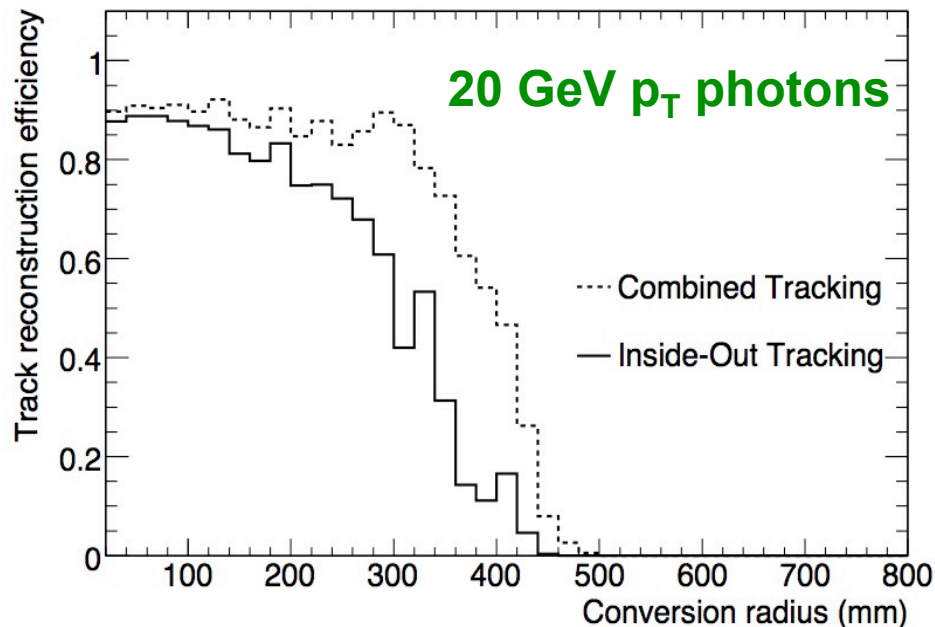
- At this point a number of TRT hit patterns have been found from the TRT straws crossed
- A second step is necessary to further process these nascent TRT track segments
- Due to their large number some selection needs to be applied, based on the number of hits
 - Only patterns with $N_{\text{hits}} > N_{\text{cut}}$ (where $N_{\text{cut}} = 9$) will be retained
- A local pattern recognition then takes place where the TRT hit drift time information is used
- Helix parameters are first defined using the best ϕ, c estimates and the $\eta(\theta)$ of the current slice
- A road is defined through the TRT detector with width 10 times the helix coordinate errors
- All straw hits are then picked up and transformed into a different coordinate system (u,v)



- Straw hits follow straight lines in the (u,v) plane
- Straw drift-time hits also follow similar pattern
- Best track segment the one that goes through most
- Best track parameters those that achieve that
- Perform final track fit using the Kalman formalism

Outside-in Track Reconstruction: Si Extensions

- Mask all Si space points that have already been used by the inside-out tracking sequence
- Remaining Si space points are ordered in small R - ϕ wedges along η
- Seeds are searched within a (R, ϕ) range indicated by the TRT segment parameters
 - Search is confined within the last three SCT layers
 - Seeds are made of two Si space points
 - One full layer hole can be allowed within the seed
 - Cut on the curvature is applied with the third point provided by the first TRT segment hit
- Better track parameter estimation after Kalman filtering through the seed
 - Improves the longitudinal component estimation
- Use new track parameters to compute a road through the Si tracker
 - Collect all possible Si detector elements and the corresponding clusters
- Use combinatorial Kalman filter/smoothing method, as in the inside-out tracking sequence

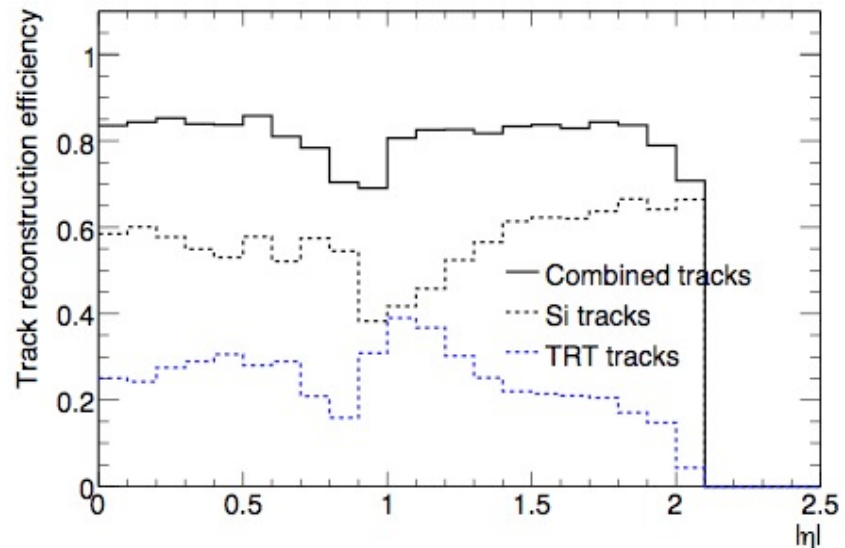
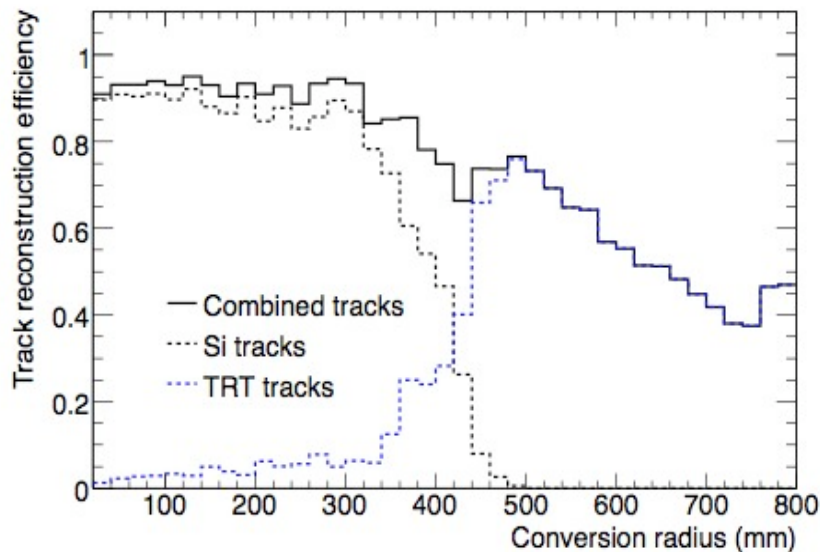


- Use new track parameters from Si extension to compute a new TRT extension
 - Identical to one used for inside-out tracking
 - No scoring involved
- Ambiguity resolving like the inside-out tracking
- **Improved efficiency at higher Si tracker radii**

Stand-alone TRT Track Reconstruction

- All unused TRT segments are transformed into tracks, called TRT-only tracks
 - A pseudo-measurement is added at the beginning of the track:
 - Contains z, θ parameter information to assist for later track fitting
 - Helps track fitters to easily converge on the fitted longitudinal parameters
- Segments with less than an η -dependent minimum number of hits are dropped
- Tracks are scored, primarily on the number of hits vs. that of expected
- Tracks are ambiguity resolved after ordering according to scoring:
 - Keep register of used TRT drift circles by already existing segments
 - TRT-only tracks that contain $>30\%$ of shared hits with other tracks are dropped
- Track parameters are provided after a final fitting

Contribution of TRT-only tracks in the track reconstruction efficiency



20 GeV p_T photons

Track Fitting

- A track fit provides the best estimation of track parameters with respect to a reference surface
 - A collection of hits is necessary to define the track trajectory
 - The reference surface is normally the perigee surface
- Various types of inputs for the hits are foreseen
 - Un-calibrated hits, i.e. raw measurements using the individual sub-detector calibration scheme
 - Calibrated-on-track hits based on the track direction and the sensor intersection point
- Necessary to define a particle type hypothesis for material effects integration
- Outlier steering logic necessary for specifying the fitting procedure
- Update the predicted track parameters after incorporating a new measurement:
 - Based on either a covariance or a weight matrix approach (later faster in execution)
- Several track fitters available; two of them of general purpose:
 - Kalman Fitter (KF)
 - Global χ^2 fitter (GXF)
- Dedicated fitters for electrons for bremsstrahlung corrections will be described separately
 - Gaussian Sum Filter (GSF)
 - Dynamic Noise Adjustment (DNA)
 - Calorimeter-based bremsstrahlung corrections (CaloBrem)

Track Fitting

- **Kalman Fitter (KF):**

- Straightforward implementation of the Kalman filter technique in track fitting
 - Initial track parameters are determined from the seed
 - Propagate to the next detector element surface, determine track parameters
 - Incorporate the measurement and update the track parameters and covariances
 - Using the updated track parameters move on to the next detector element
- Combines a forward filtering, backward smoothing and outlier handling techniques
 - The final track parameters are defined only after all the above
 - Backwards smoothing starts with the track parameters from the filter step
 - Backwards smoothing essential for final decision on outliers and holes
- A detailed description of the Si tracker geometry is used throughout
 - Careful handling of material effects e.g. multiple scattering and ionization
 - Extension of the KF to handle bremsstrahlung losses (DNA) will be described later

- **Global χ^2 Fitter (default track fitter):**

- Track fitting is done through the minimization of a global χ^2 value
 - Main assumption is purely Gaussian process noise
 - The χ^2 is built from the hit residuals at every measurement surface
 - Minimization of this χ^2 marks the best estimation of the track trajectory
- Material effects enter the χ^2 function as additional fitting parameters
 - Weighted by their expected variance due to their stochastic nature
- Minimization of global χ^2 is performed by solving a set of linear equations (matrix inversion)
 - Number of global parameters needs to be kept small to minimize CPU time consumption

Tracking Performance

- Use precise modeling of individual detector response, geometry and passive material
- Particles originating at the primary vertex with $p_T > 1$ GeV and $|\eta| < 2.5$ considered
- Use standard quality cuts to select tracks:
 - Tracks are required to have at least 7 Si clusters
 - Transverse impact parameter $|d_0| < 2\text{mm}$
 - Longitudinal impact parameter $|z_0 - z_v| \times \sin\theta < 10\text{mm}$, z_v primary vertex position along beam

- Resolution for a track parameter X can be expressed as:

$$\sigma_X(p_T) = \sigma_X(\infty) (1 \odot p_X/p_T) \text{ where}$$

$\sigma_X(\infty)$: asymptotic resolution at infinite momentum

p_X : a constant representing the value of p_T for which intrinsic and multiple scattering terms for track parameter X are equal

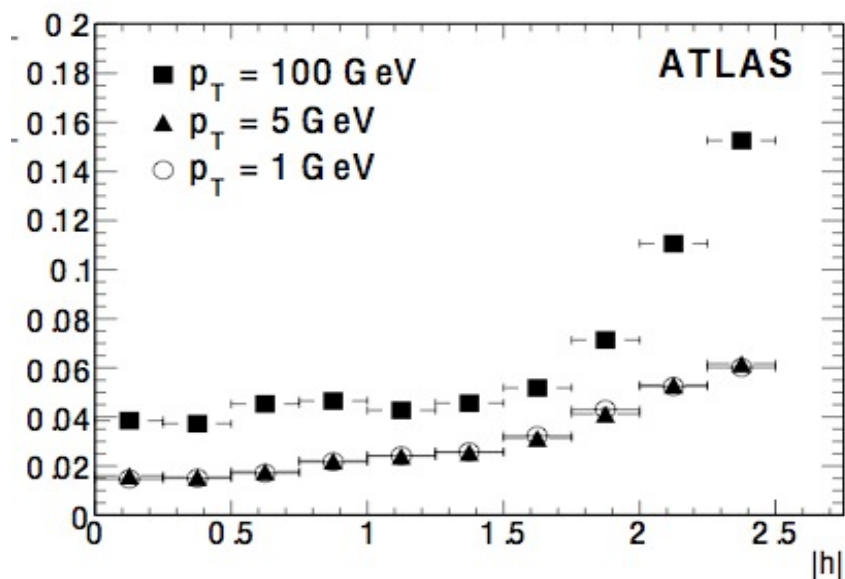
\odot : denotes addition in quadrature

$\sigma_X(\infty)$ and p_X are implicit functions of pseudorapidity η

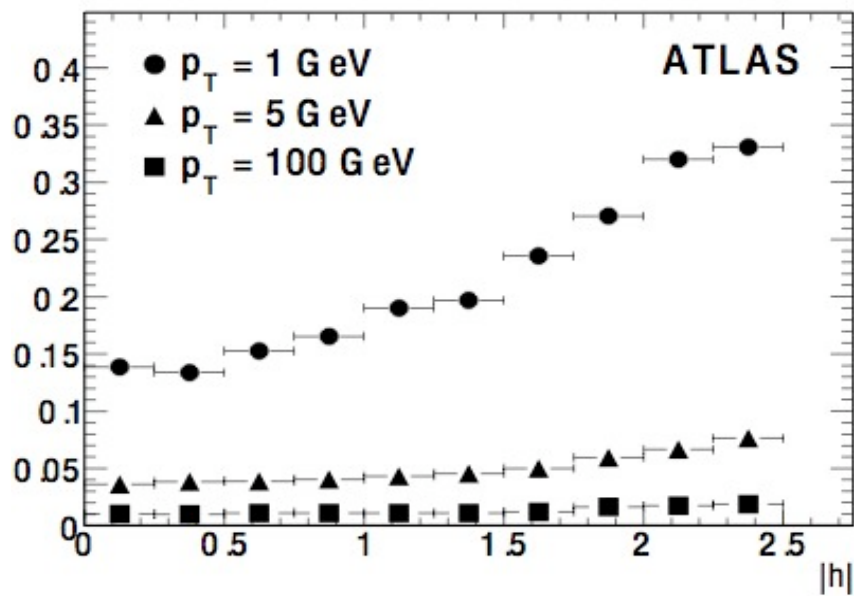
- Resolutions are defined as RMS values corresponding to $\pm 3\sigma$ range around the mean value
- Perfect alignment of the tracker is assumed
- TRT measurements are included for all tracks with $|\eta| < 2.0$

Track parameter	$0.25 < \eta < 0.50$		$1.50 < \eta < 1.75$	
	$\sigma_X(\infty)$	p_X (GeV)	$\sigma_X(\infty)$	p_X (GeV)
Inverse transverse momentum ($1/p_T$)	0.34 TeV^{-1}	44	0.41 TeV^{-1}	80
Azimuthal angle (ϕ)	$70 \mu\text{rad}$	39	$92 \mu\text{rad}$	49
Polar angle ($\cot \theta$)	0.7×10^{-3}	5.0	1.2×10^{-3}	10
Transverse impact parameter (d_0)	$10 \mu\text{m}$	14	$12 \mu\text{m}$	20
Longitudinal impact parameter ($z_0 \times \sin \theta$)	$91 \mu\text{m}$	2.3	$71 \mu\text{m}$	3.7

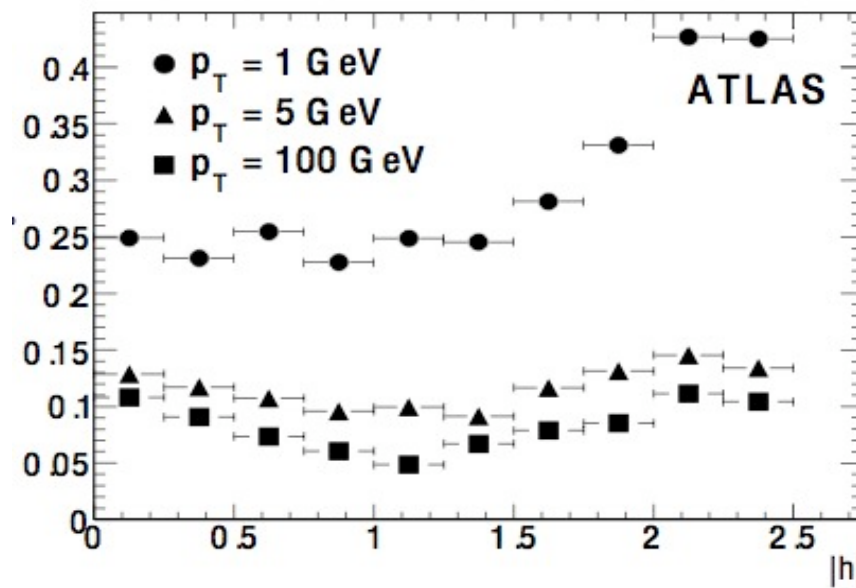
Tracking Performance



Relative p_T resolution for muons vs. the pseudorapidity η

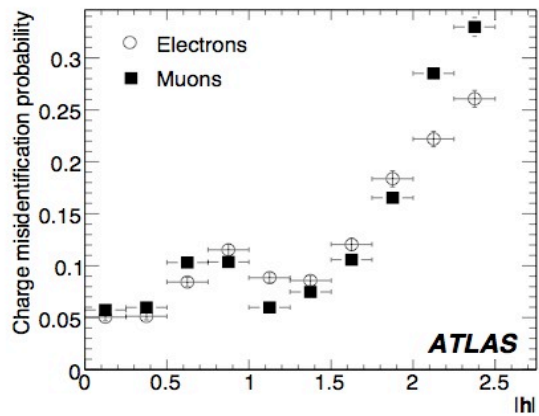
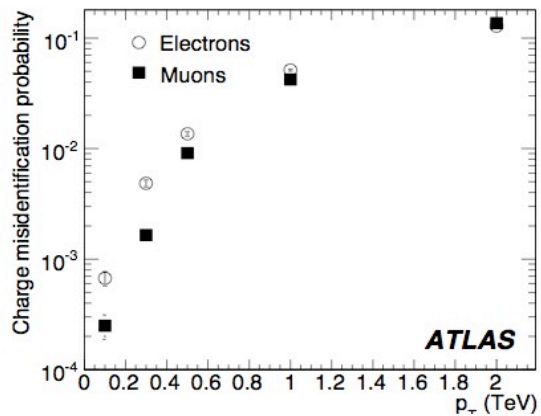


Impact parameter d_0 resolution for pions

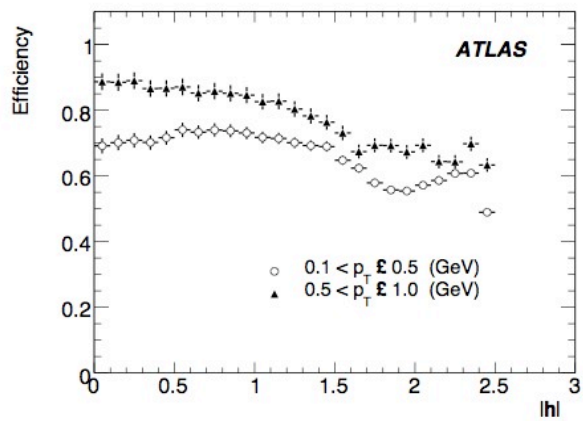
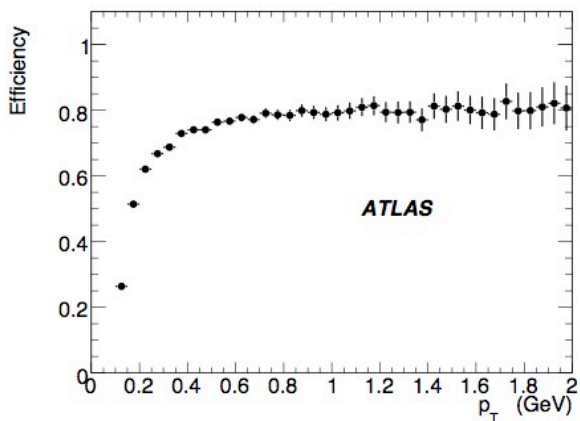


Modified impact parameter $z_0 \times \sin\theta$ resolution for pions

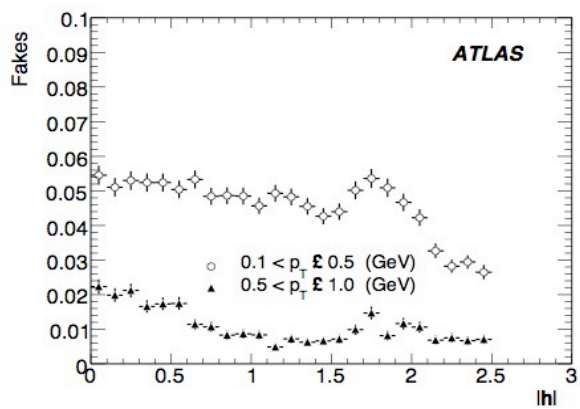
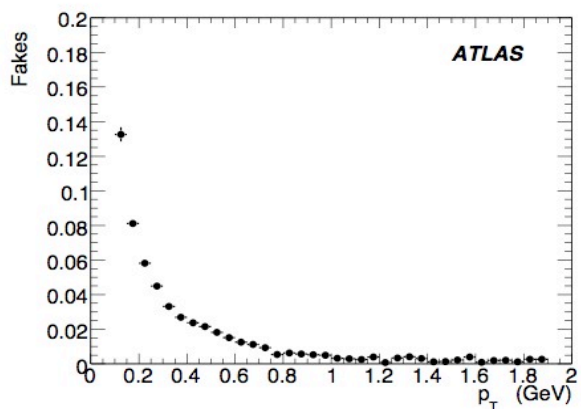
Tracking Performance



Charge misidentification

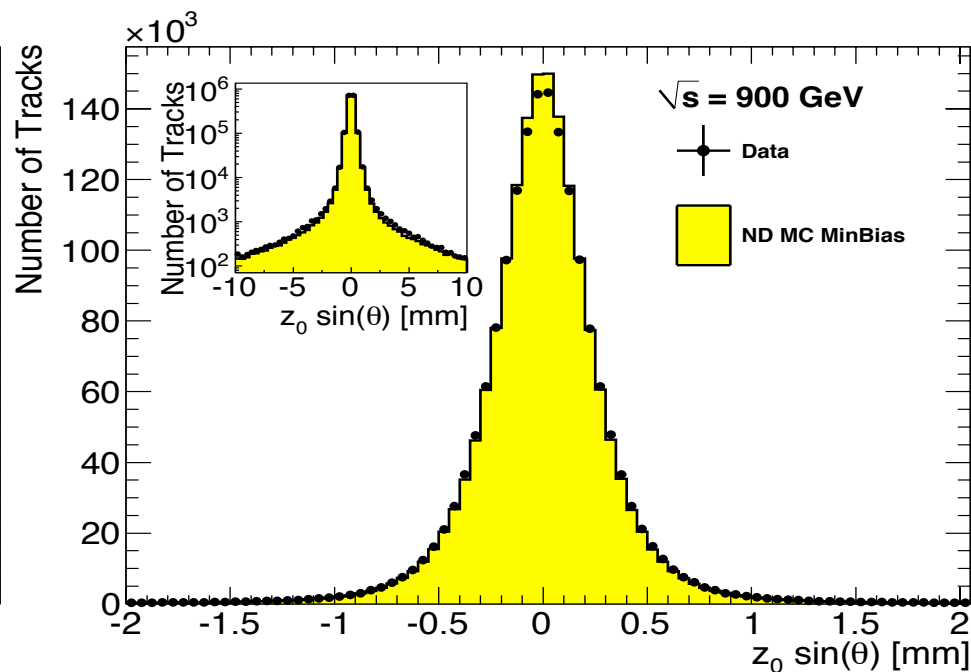
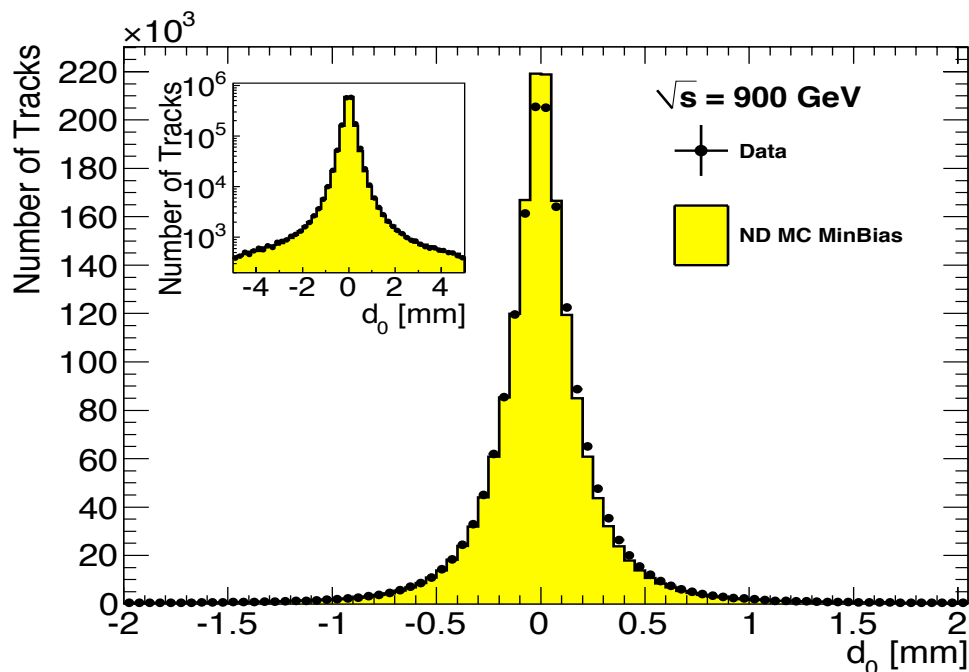
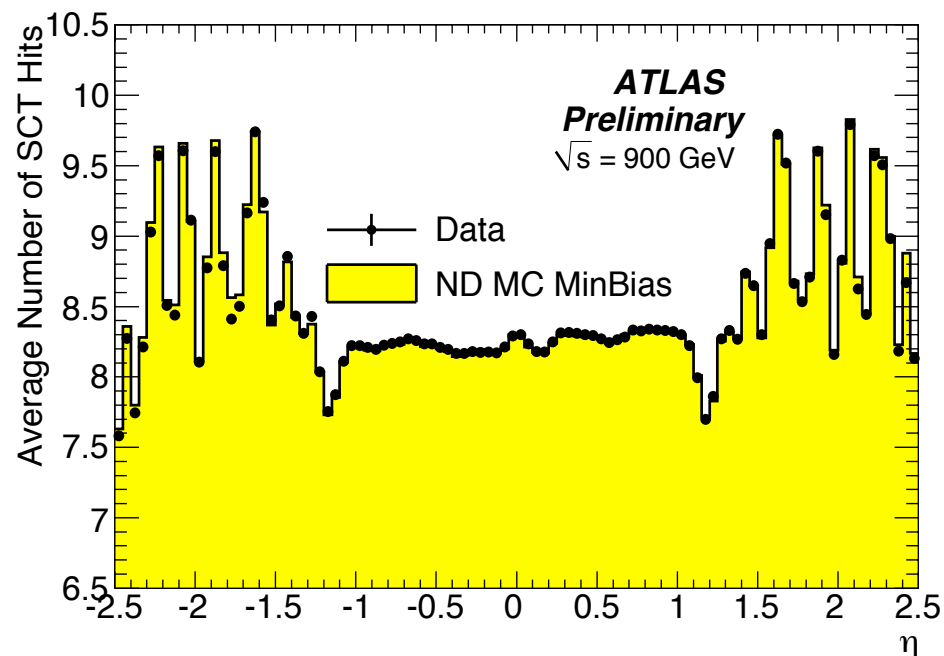
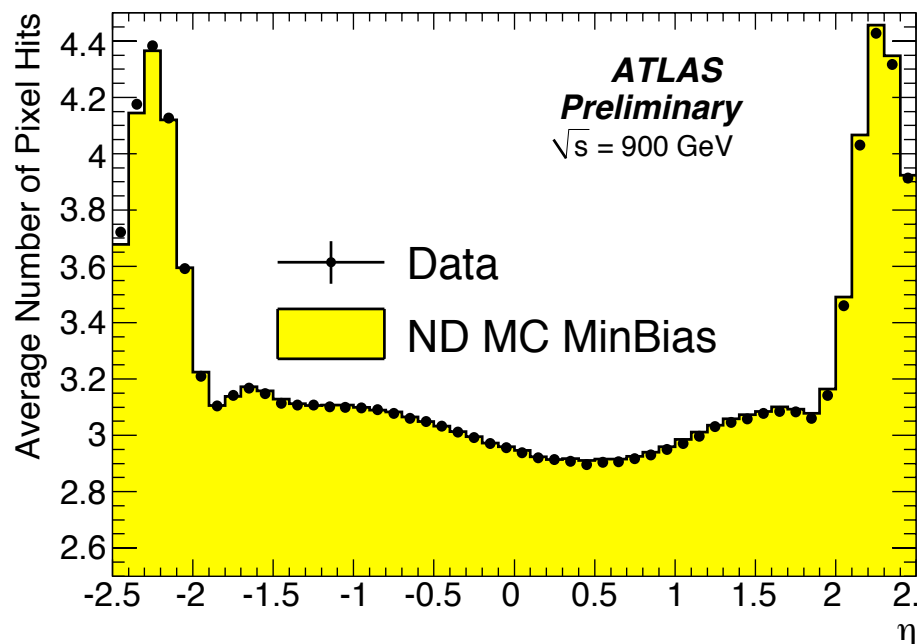


Track reconstruction efficiencies for minimum bias events



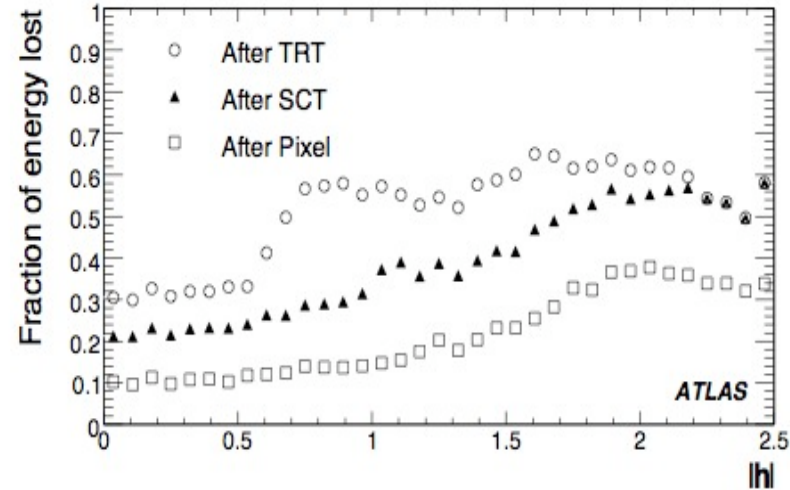
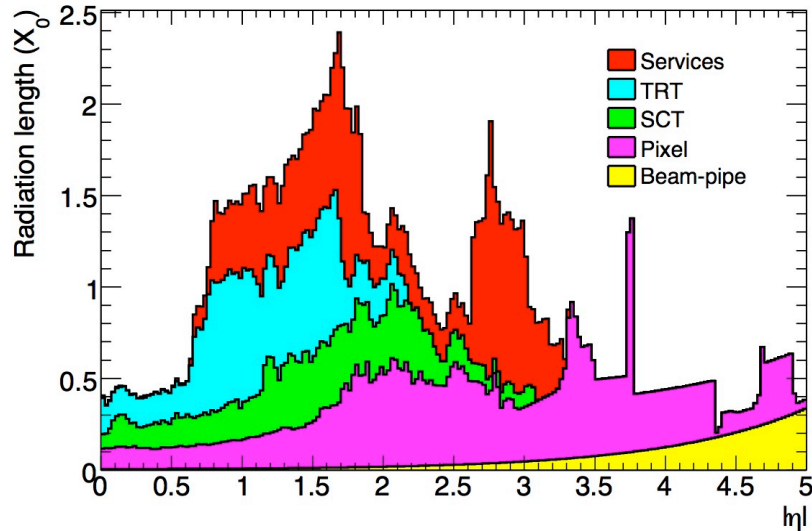
Fake rates in minimum bias events

Tracking Performance: 900 GeV Minimum Bias Data

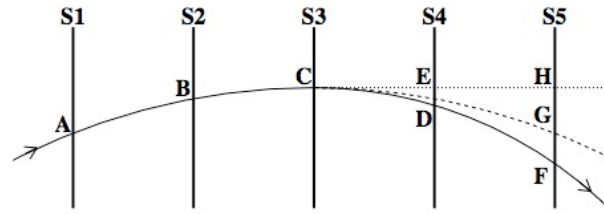
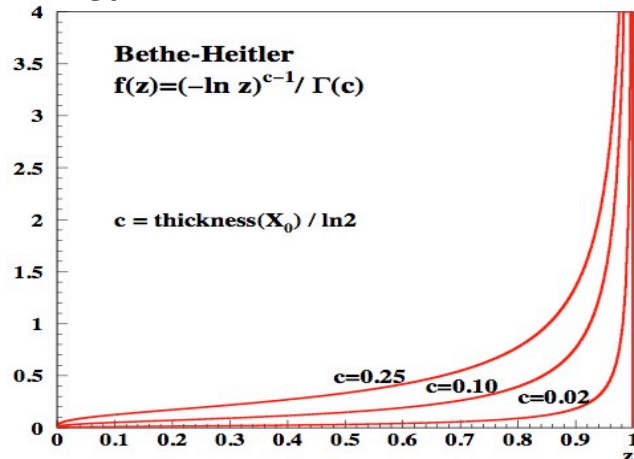


Electron Track Reconstruction

- Reconstruction of electrons (and converted photons) a particular challenge in ATLAS
 - Unprecedented amount of material in tracker traversed by electrons



- Transition Radiation Tracker (TRT) provides particle identification capabilities
 - Separation of electrons from pions or muons possible
- Track or calorimeter based bremsstrahlung recovery algorithms improve track parameters
- Energy loss due to bremsstrahlung described by Bethe-Heitler



Electron retains its direction of propagation

Dynamic Noise Adjustor

- An extension of the Kalman Filter
- As energy losses due to bremsstrahlung are not modeled well by a single Gaussian another method is required to incorporate them.
- At each layer a single parameter fit is performed to indicate the presence of the bremsstrahlung
- If no bremsstrahlung candidate is detected, standard Kalman Filtering is used
- In the case of bremsstrahlung activity the fit result is used to estimate the energy fraction retained, z , which is then used to calculate the effective system noise.

$$\sigma_{DNA}(z) = \frac{\Delta z}{\Delta x}$$

- This noise term is then added to the Kalman covariance matrix of the fit

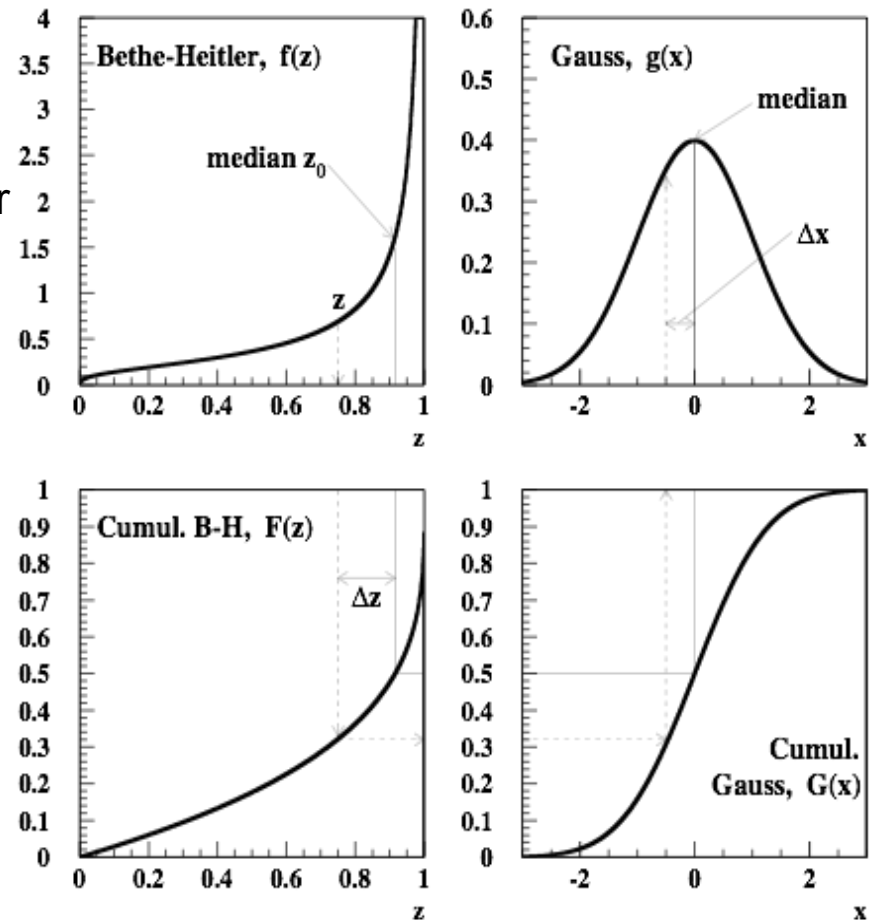
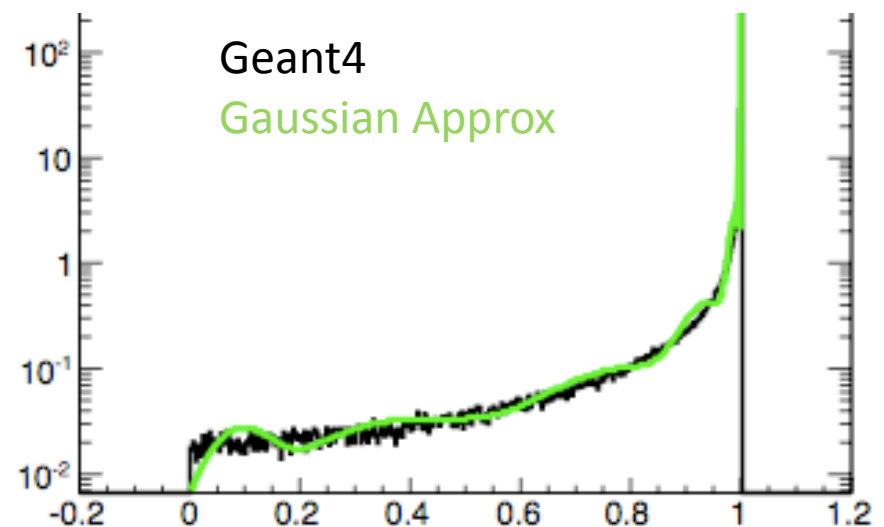
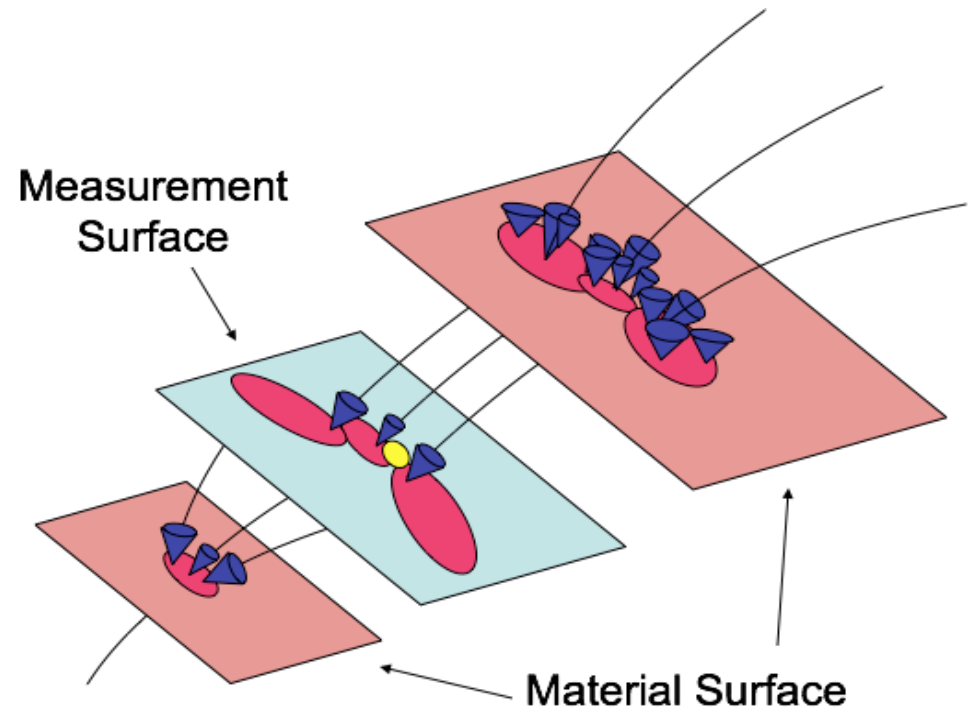


Figure 4. Mapping of probability distributions used to calculate the variance of the effective noise term.

V. Kartvelishvili and ATLAS Collaboration, Electron bremsstrahlung recovery in ATLAS, [Nucl. Phys. Proc. Suppl. 172, 208 2007.](#)

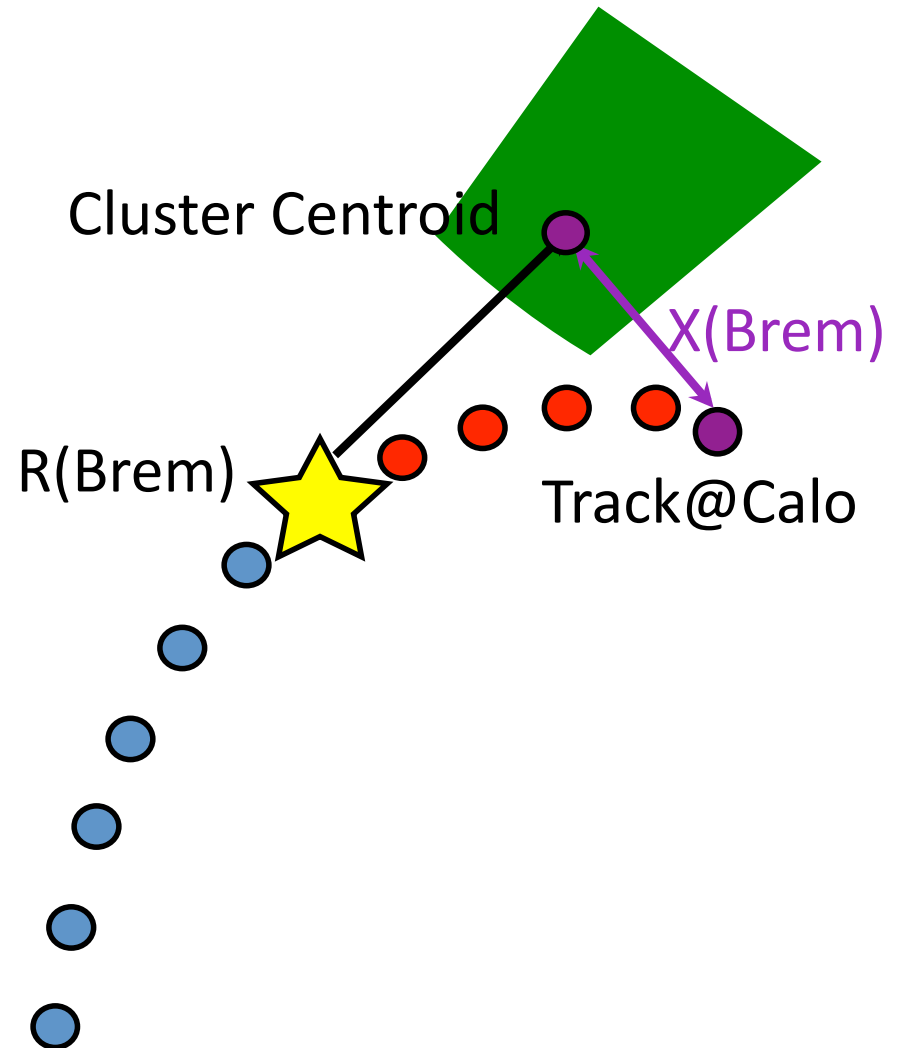
Gaussian Sum Filter

- Generalization of the Kalman filter
- Can be thought of as a series of KF's working in parallel
- Track parameters PDF represented by weighted sum of Gaussian's.
- At each material layer the track parameters are convolved with a PDF describing the material effects
- To ensure that number of Gaussians in the PDF does not explode they are limited.



CaloBrem

- A track fit that incorporates the position of the electromagnetic cluster into the track fit.
- The position of the cluster is on the path of the original track if all energy from the original electron is located in the cluster.
- Track model is modified to include a single loss of energy at a certain radius.
- The key to a stable fit is that the cluster be included in the fit
- The track model is inherently non-linear and as a result requires an iterative track fit.
- TMinuit is used to minimize the χ^2 of the track.



Brem Effects

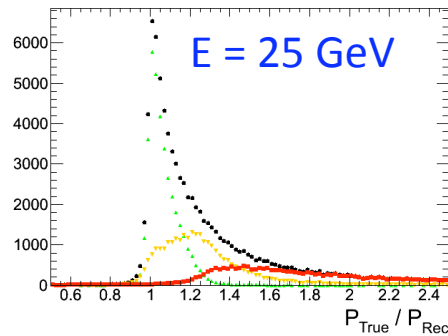
All Tracks

Hard Brem = Lost >20% of Energy in a Single Brem & $r < 300\text{mm}$

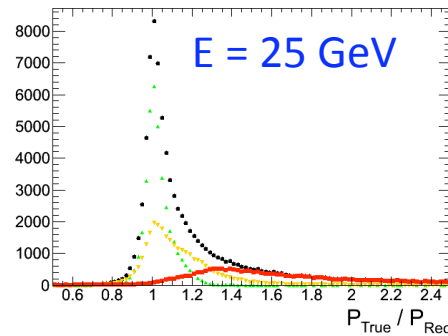
Medium Brem = !Hard or !Light

No/Light Brem = Lost < 20% of energy while $r < 600\text{mm}$

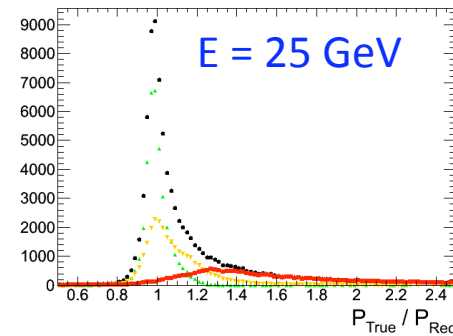
Default



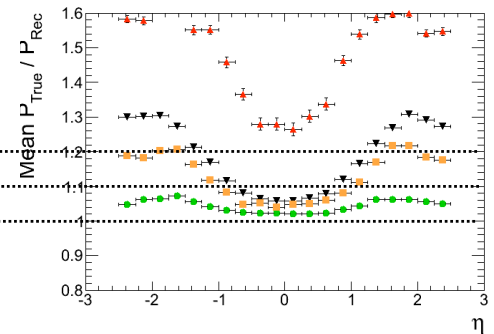
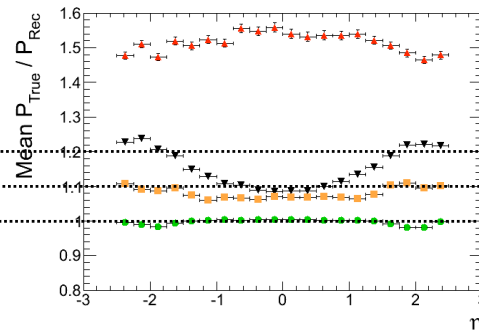
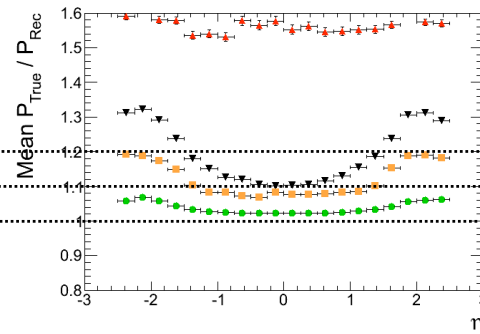
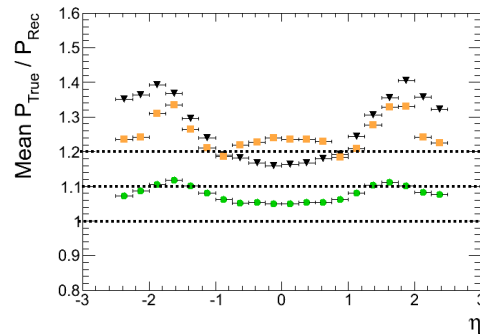
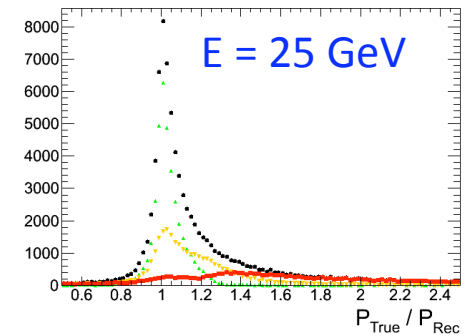
DNA



GSF

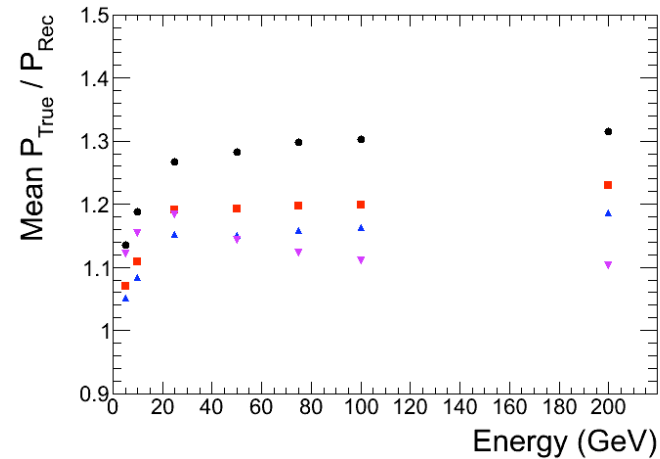
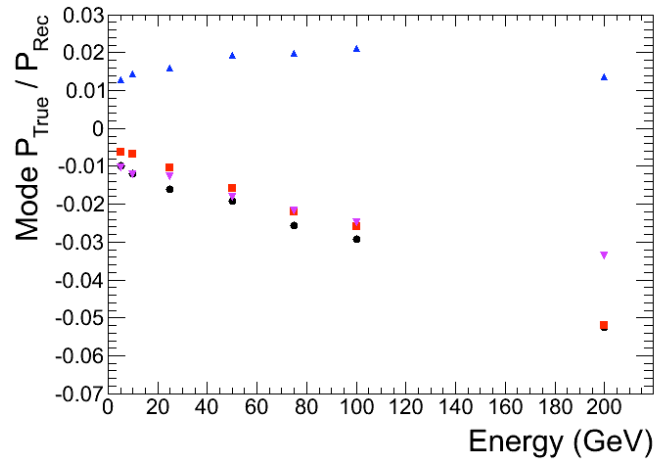


CaloBrem

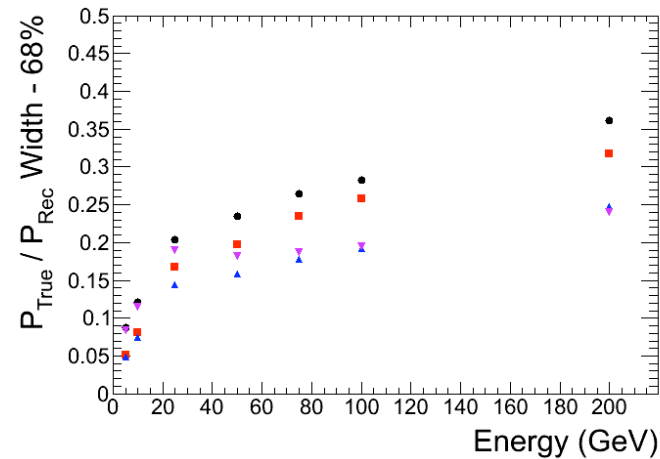
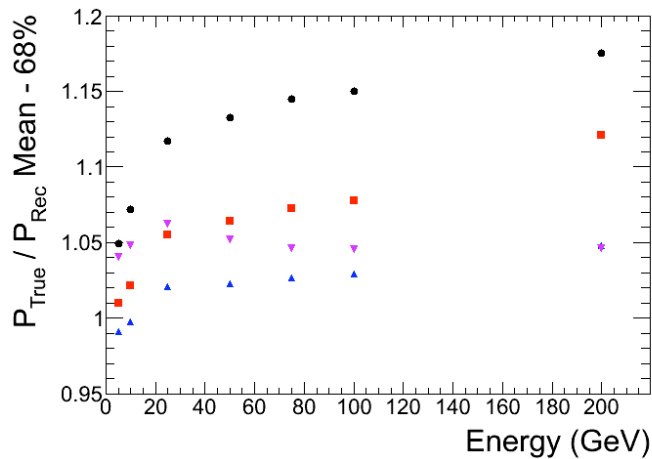


- Definition of Brem classification are made to highlight the effects on tracking
- DNA and GSF make a significant improve to Medium Brem (Peak shift from 1.2 ->1.0)
- GSF looks particularly linear as a function of η for the No, Medium and Hard Brem events. This is very dependent on the definitions of the classifications
- CaloBrem shows major improvement on Hard and Medium events when in the central barrel (The region of significant improvement increase with E)

Default
 DNA
 GSF
 CaloBrem



All Events

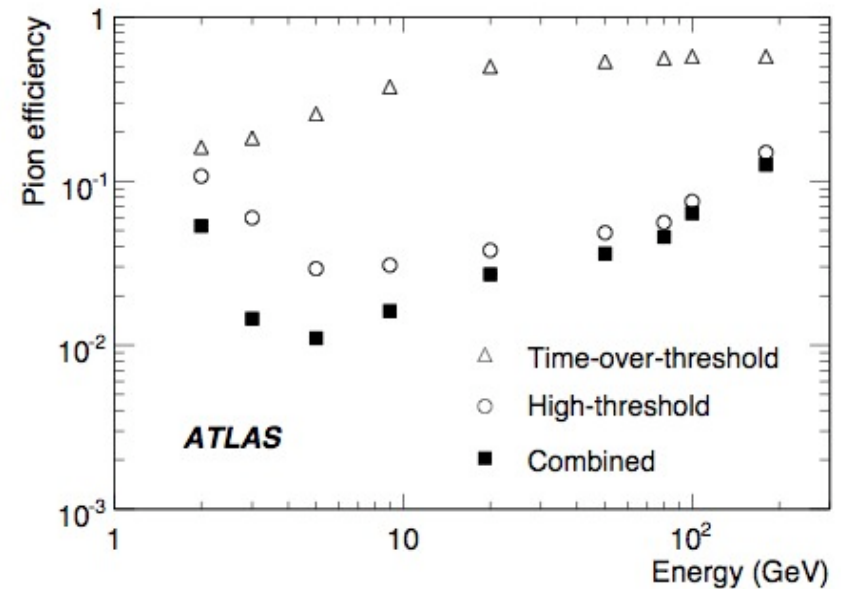
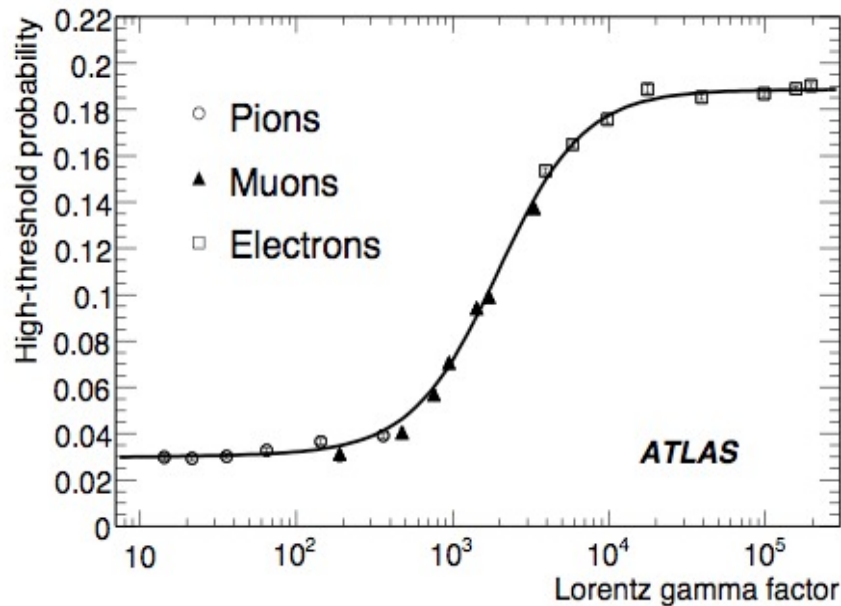


Narrowest
 windows to
 contain 68%
 of events

- The effect of looking at reconstructed electron tracks on the tracking can be seen in the mean. When $E > 25$ GeV a significant fraction of the hard bremsstrahlung events are not reconstructed as electrons; as a result the mean of $P_{\text{True}}/P_{\text{Rec}} > 1$
- The Mode of the distribution was obtained by a Crystal ball function fit to the data.
 - Peak of GSF overestimate the energy by 1-2%
 - All other fitters underestimate by varying degrees (-0.5% -> -5%)
- The performance of CaloBrem as expected improves as the energy increase. Significant improvement above 10 GeV. Near Parity with DNA at 25GeV

Electron Identification

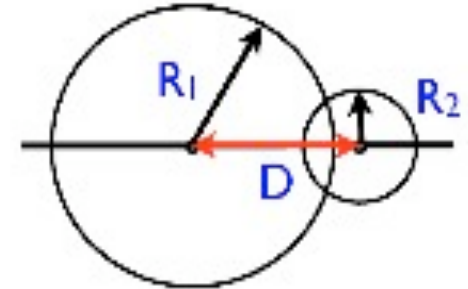
- Transition radiation X-rays contribute significantly to the number of high threshold hits
 - True for electrons with energies above 2 GeV
 - Saturation sets in at electron energies above 10 GeV
- Set up a likelihood evaluation based on the high threshold probability for electrons
- Including the Time over Threshold (ToT) could improve the rejection



- At low energies pion rejection improves with energy; optimal conditions at 5 GeV
- At higher energies pions become relativistic and start to emit transition radiation
- Performance in endcap TRT better than in the barrel

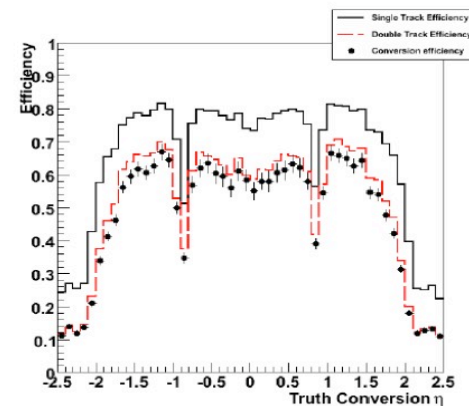
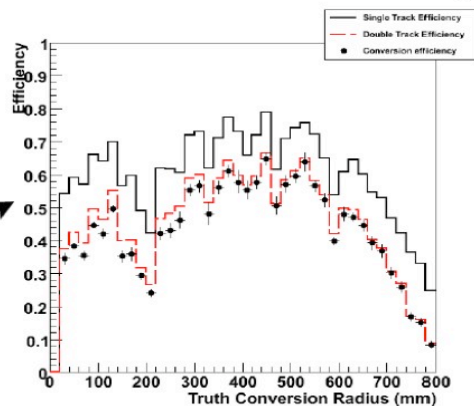
Converted Photon Reconstruction

- Tracks are selected based on their particle identification probability for being electrons
- Pairs are formed using opposite charge tracks
- Track pairs are selected according to the following criteria:
 - Distance of minimum approach between the two tracks in the pair
 - Opening angles in θ and ϕ
 - D-R1-R2 as shown in the figure
- Selected pairs are passed to the vertex fitter:
 - Constrained fit where $\Delta\theta=\Delta\phi=0$ is required (equivalent to massless particle)
 - Additional selection using the fit χ^2
- Reconstructed vertices suffering from combinatorial background



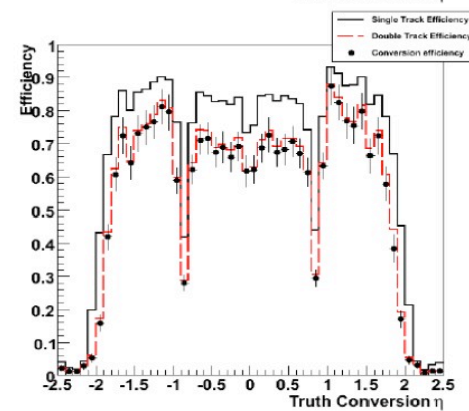
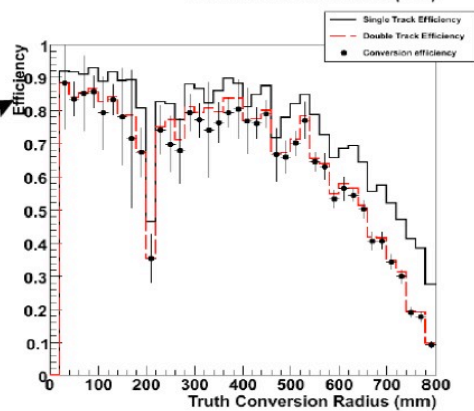
Fiducial selection:
 $R < 800$ mm,
 $|\eta| < 2.5$,
 $pT(\text{trk1}) > 500$ MeV/c
 $pT(\text{trk2}) > 500$ MeV/c

low efficiency due to
 brem in material



Vertex reconstruction
 efficiency virtually 100%

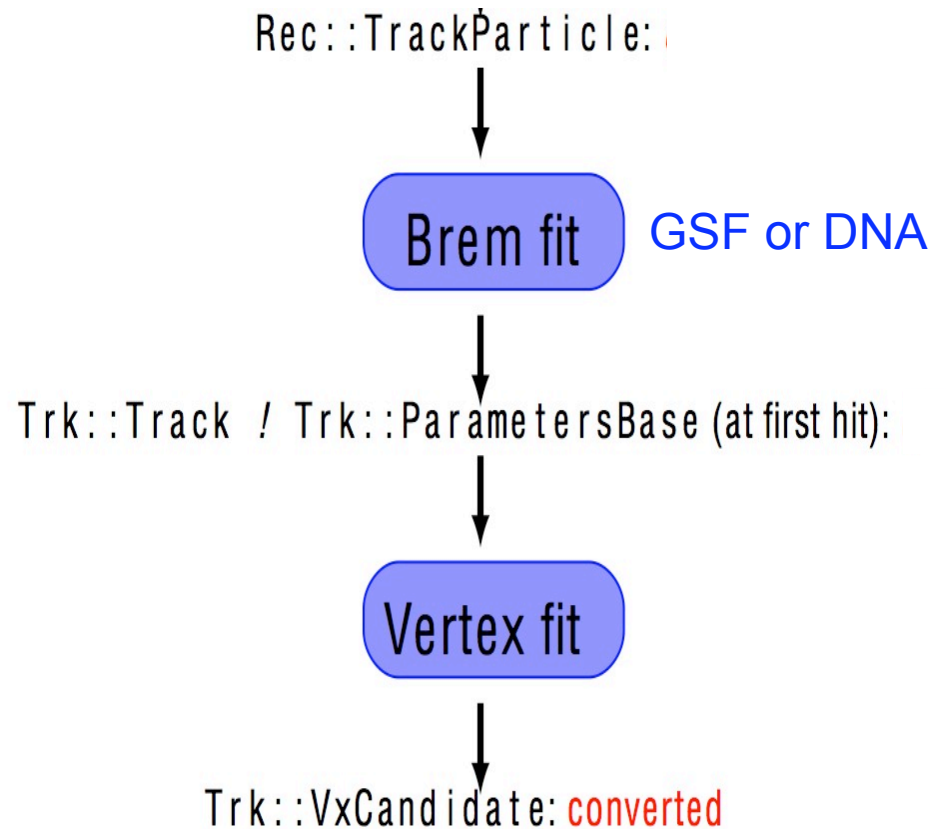
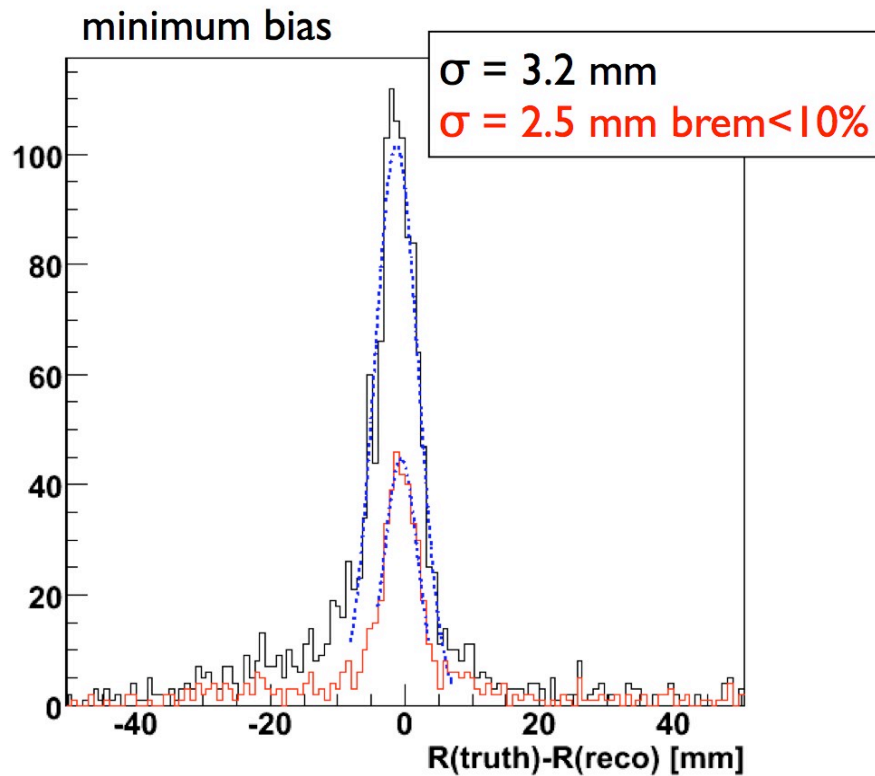
brem < 10%
 on each track



Single 20 GeV photons

Converted Photon Reconstruction

- Reconstructed conversion vertex plagued by bremsstrahlung losses:
 - Produced electrons suffer from bremsstrahlung losses like all the rest
 - Severely affects the accuracy of the reconstructed vertex radial position R
 - Severely affects the accuracy of the reconstructed converted photon p_T
- Refitting of produced electron tracks to correct for bremsstrahlung losses necessary
- Should then repeat the constrained vertex fit using the improved track parameters

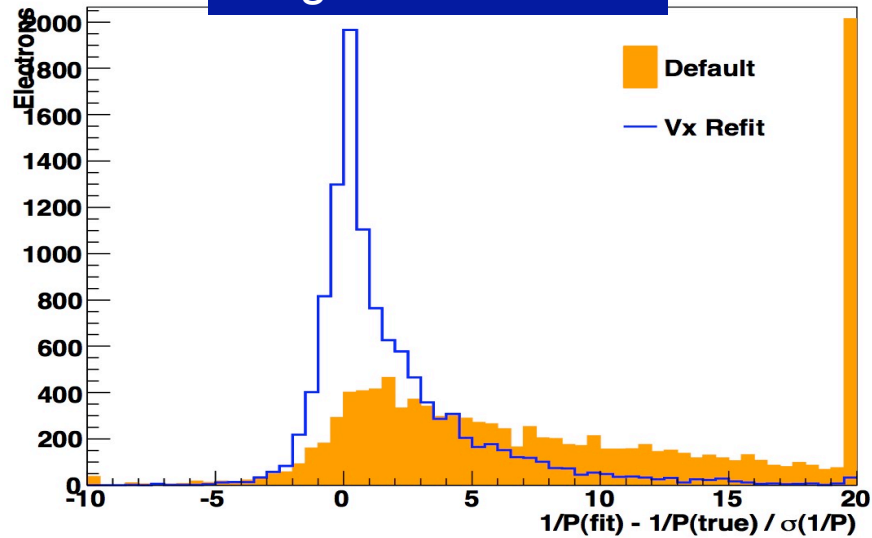


Converted Photon Reconstruction

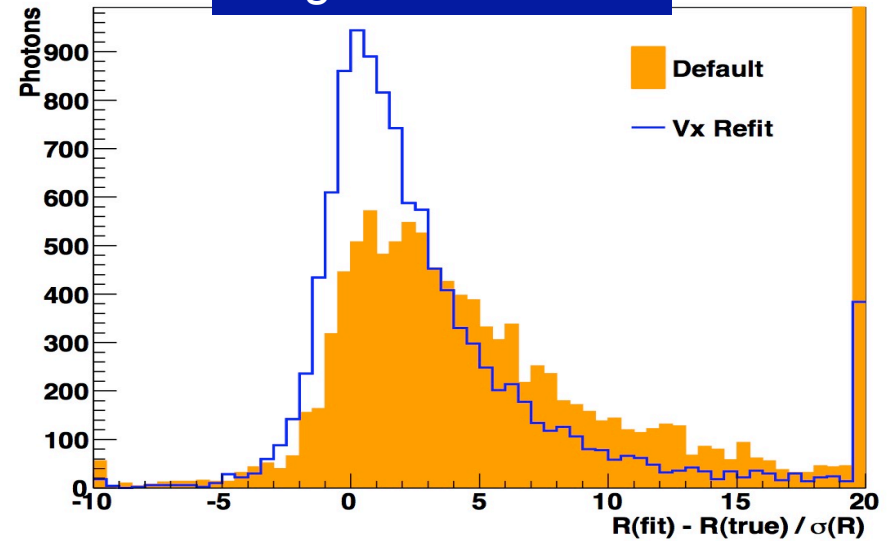
Reconstructed photon 1/p pulls (GSF)

Reconstructed vertex R pulls (GSF)

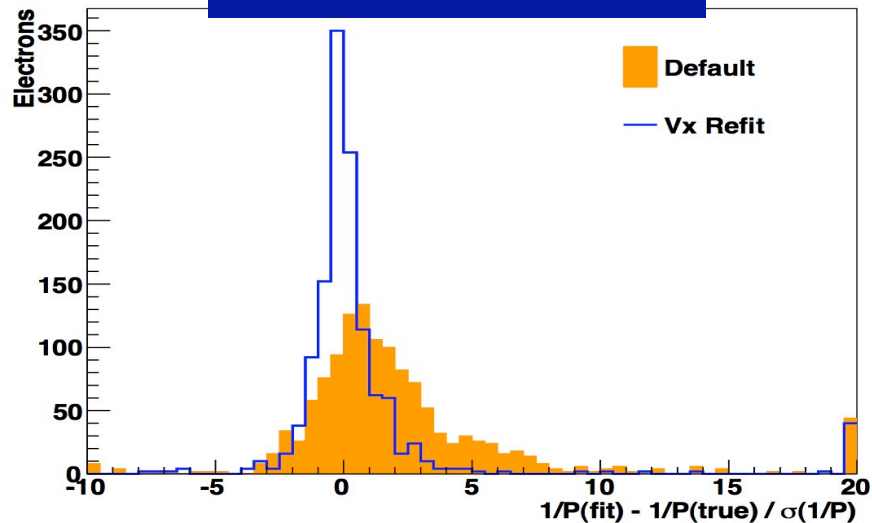
Large Brem > 40%



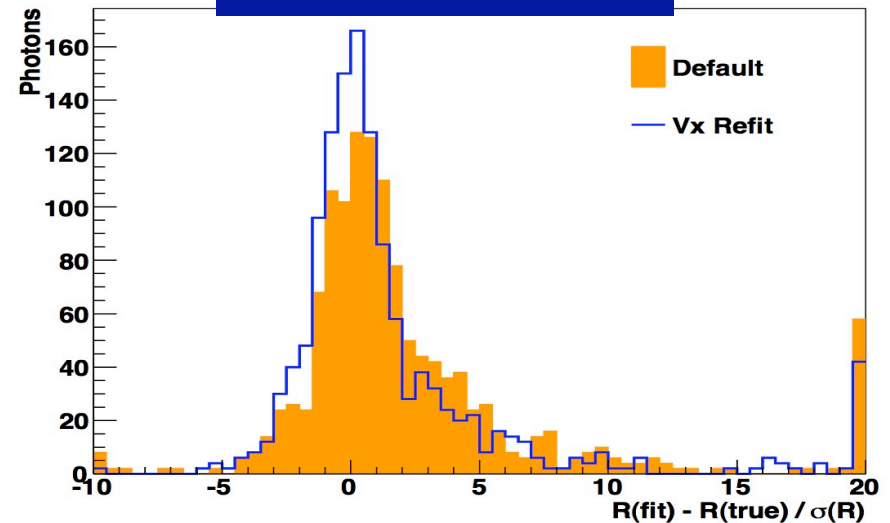
Large Brem > 40%



Small Brem < 20%

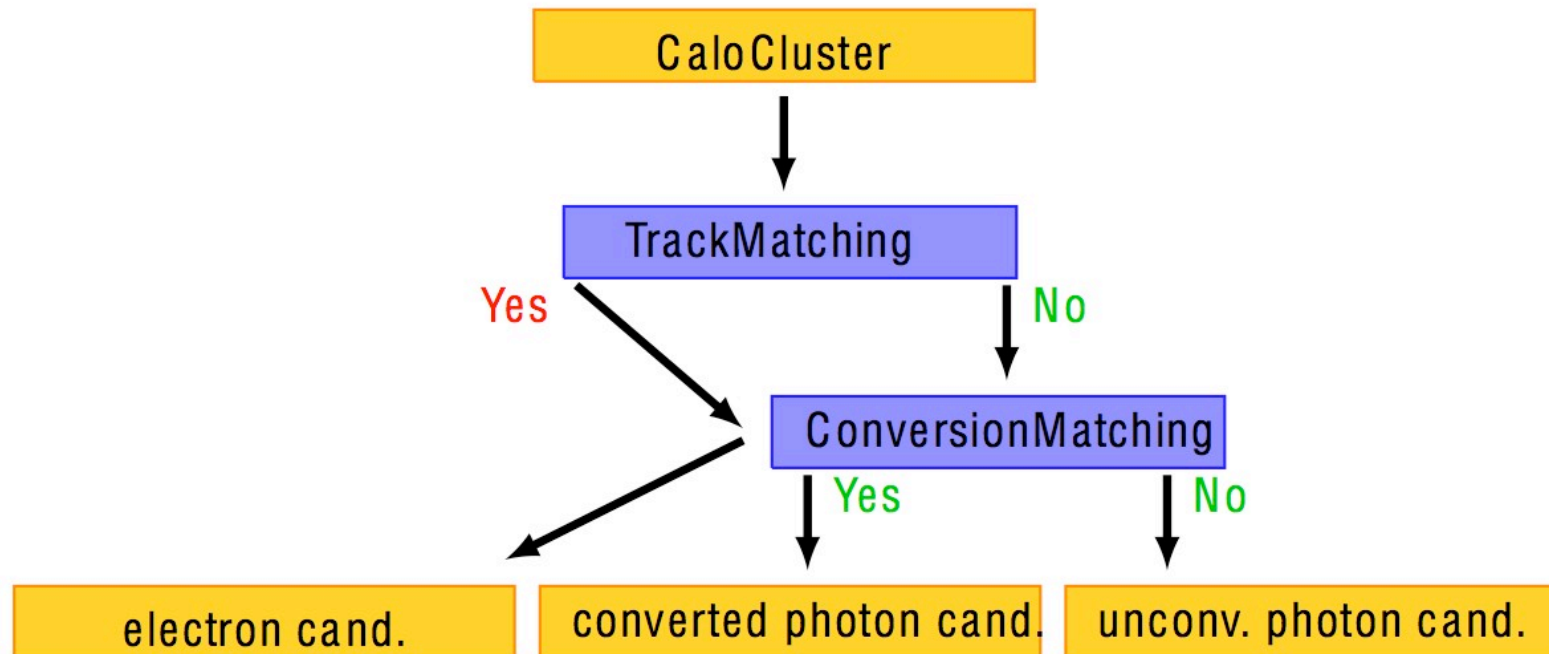


Small Brem < 20%



Combined Electron Reconstruction in e/ γ

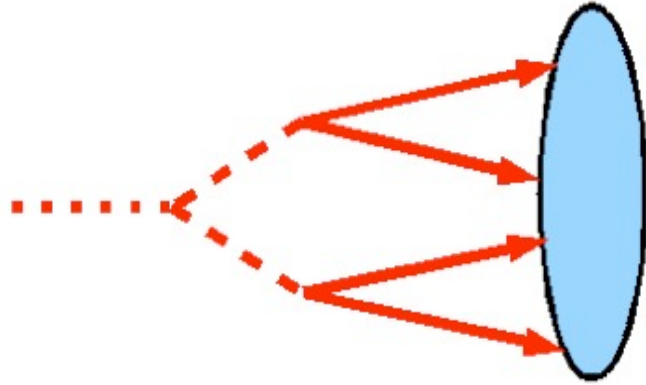
- Electrons are electromagnetic objects therefore a cluster should be assigned to them
 - The e/ γ combined performance reconstructs electrons (and photons)
 - The inputs are tracks , conversion vertices and electromagnetic clusters
- Generally a track matched to a cluster is defined as an electron object
- Similarly a conversion vertex matched to a cluster is defined as a converted photon
- Electromagnetic clusters without any tracks or vertices matched to them are unconverted photons



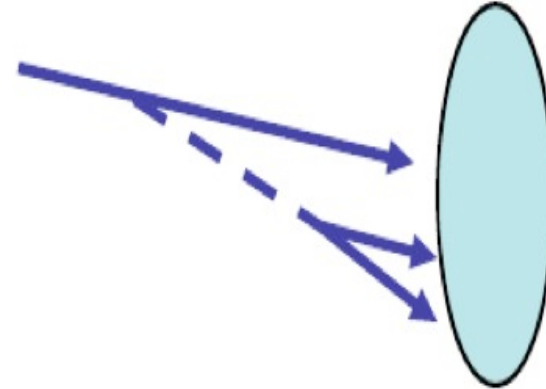
- Most converted photons are reconstructed as electrons
- Electromagnetic showering might lead to more than one track/vertex matched to one cluster
 - Multiple element links (to tracks/vertices)
 - Allows to re-visit the assignment of best track/vertex, e.g. after bremsstrahlung corrections
 - Allows to address complicated topologies

Multiple Matches to Electromagnetic Clusters

$\pi^0 \rightarrow \gamma\gamma$ with 2 converted photons



Bremsstrahlung and conversion



- Multiple links to tracks/vertices makes studying complicated topologies easier

Tracks and conversions ordered by “quality” of match

★ Follows previous egamma selection of best matches

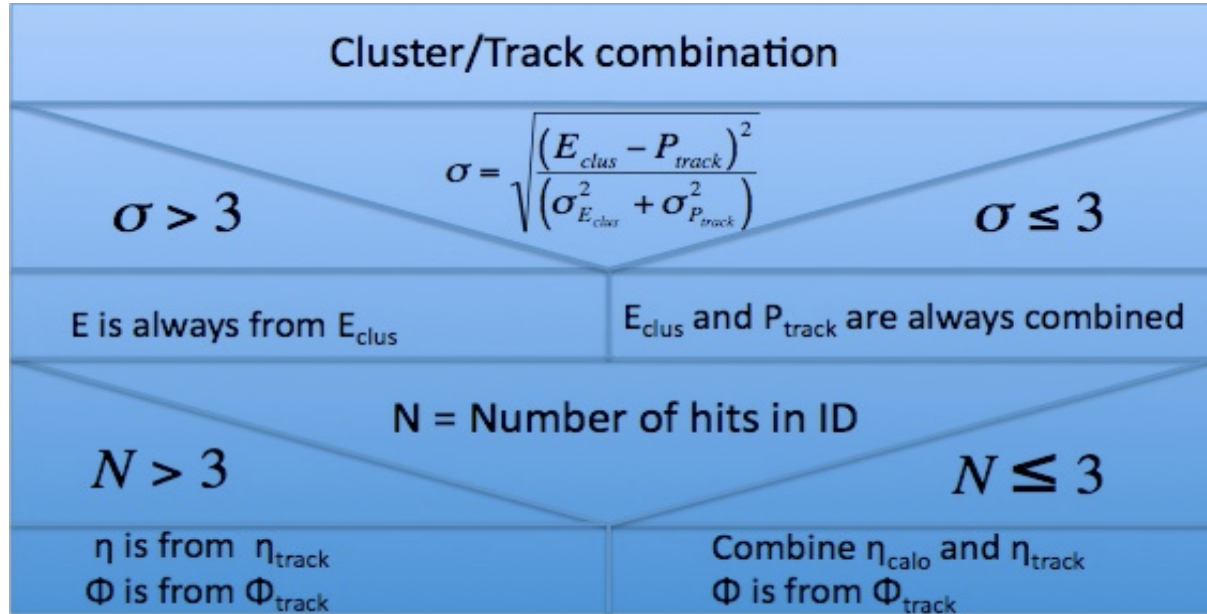
★ Tracks

1. Tracks with > 3 Si hits, ascending $\Delta R = \sqrt{(\Delta\eta)^2 + (\Delta\phi)^2}$
2. Tracks with ≤ 3 Si hits, ascending $|\Delta\phi|$

★ Conversions

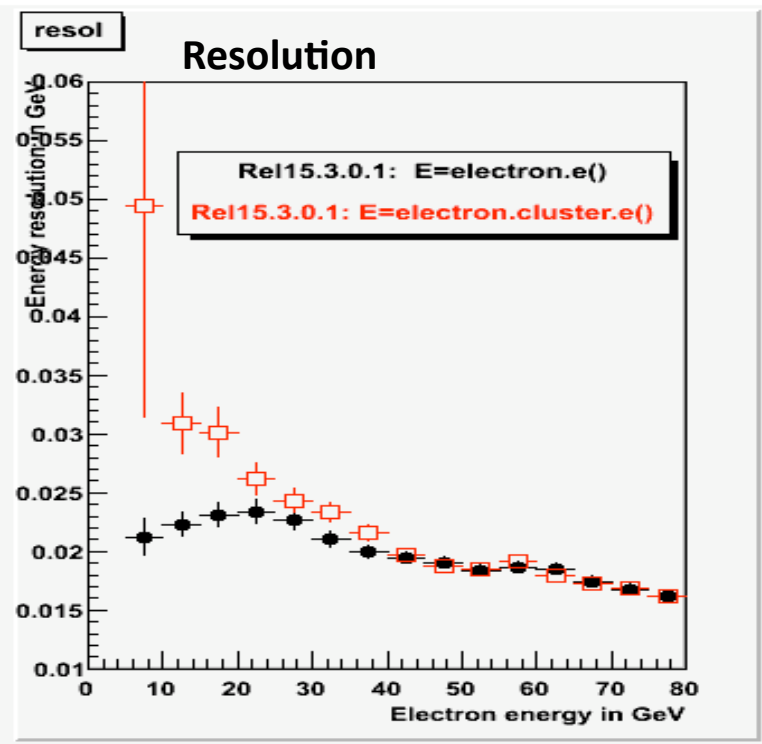
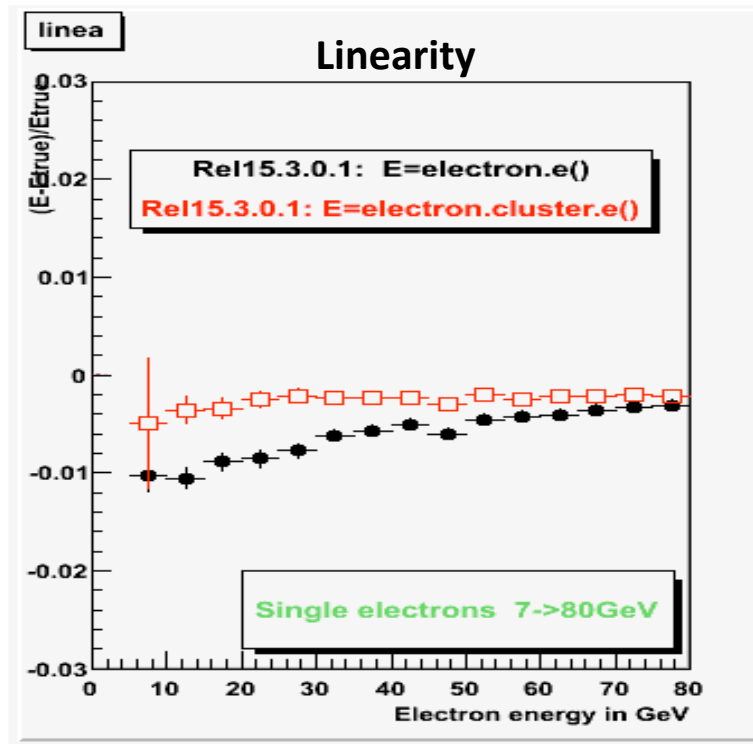
1. Double-track conversions, ascending R (conversion radius)
2. Single-track conversions, ascending R

Electron Four-Momentum

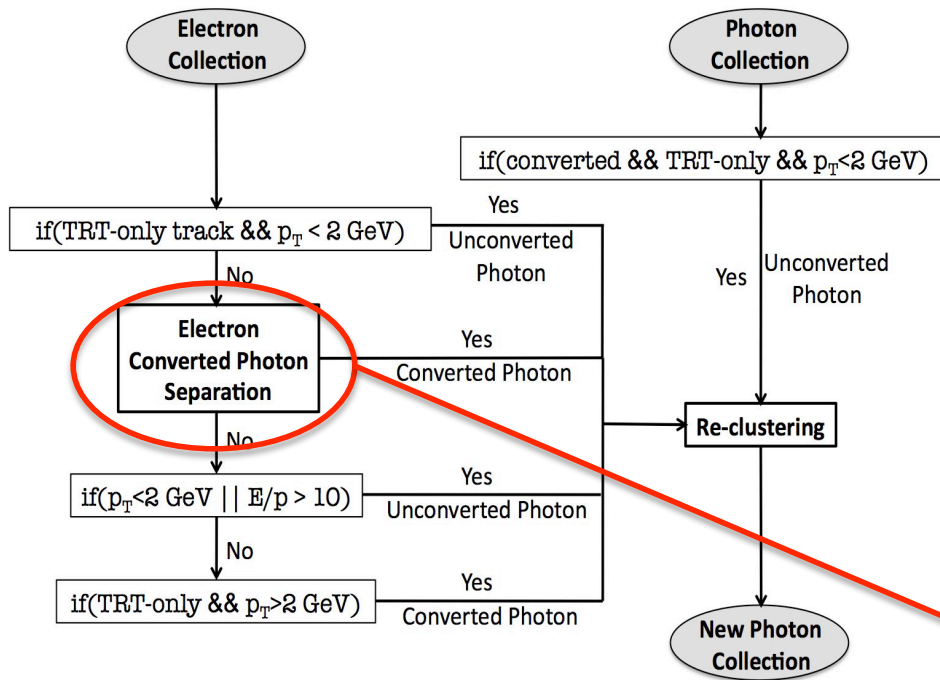


Combine tracker and electromagnetic calorimeter information to estimate energy and direction

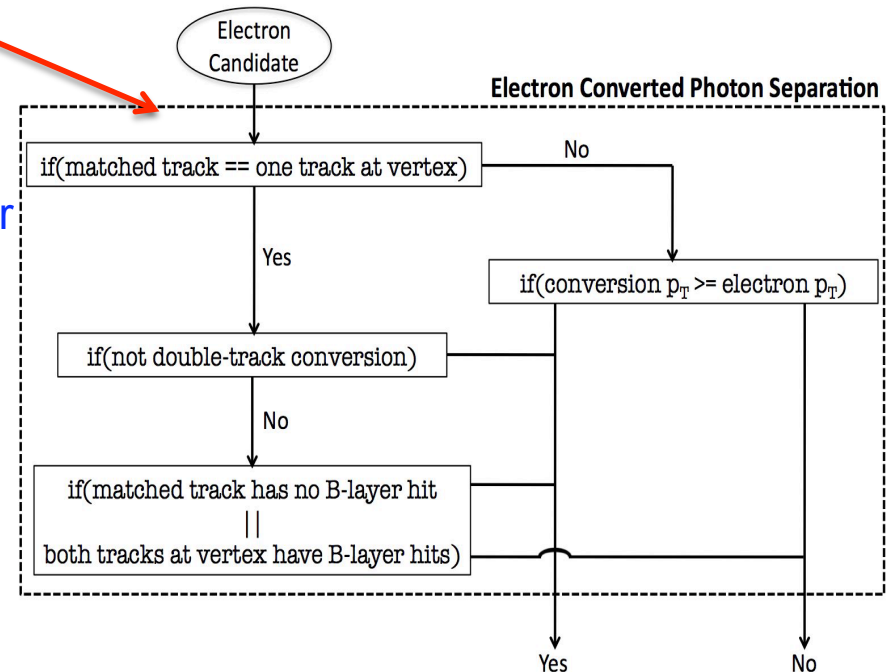
Not used yet in the case of converted photons



Photon Recovery

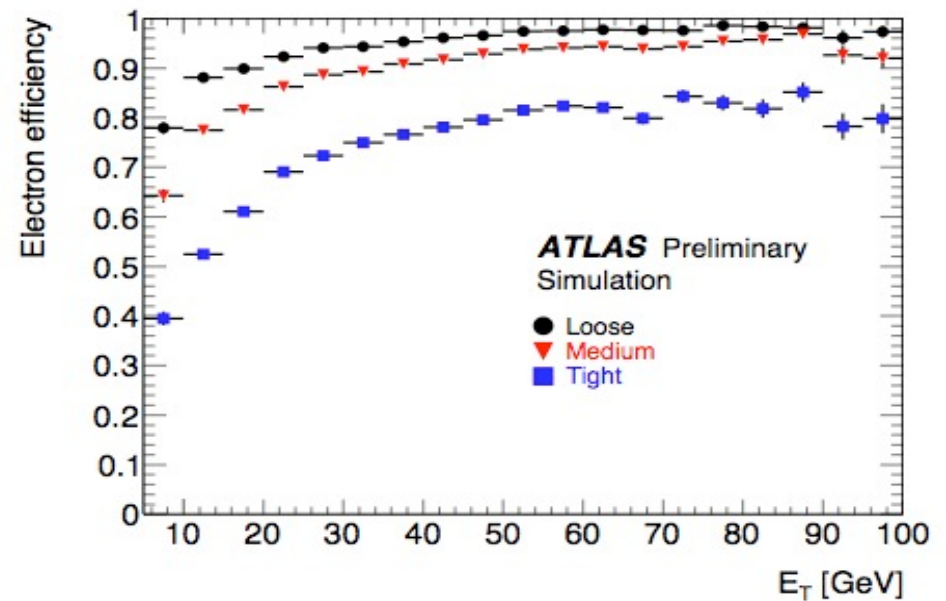
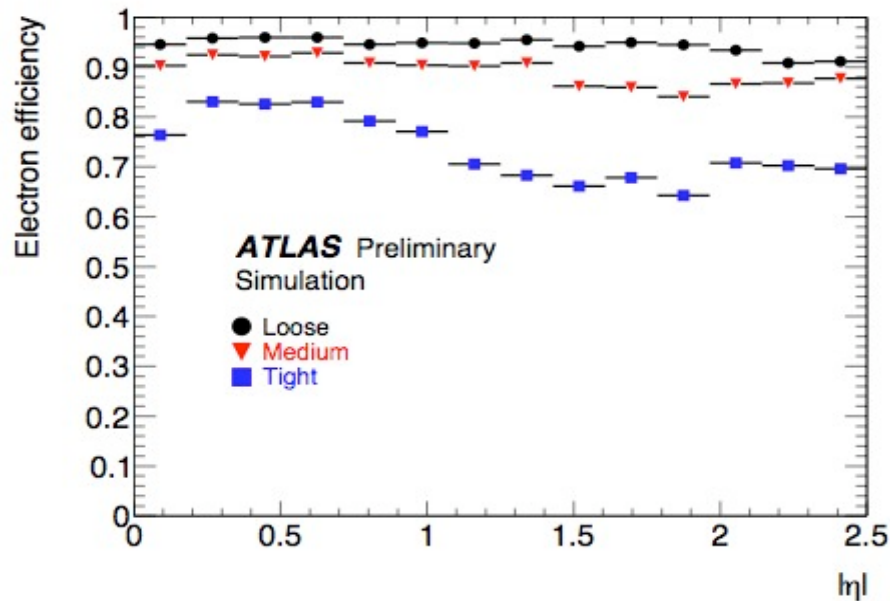


- Converted photons end up in the electron container
 - Highly unfortunate; conversions ~50% of sample
- Electron object highly ambiguous:
 - Need to separate prompt electrons from photon conversion electrons
- Ambiguity resolving re-assigns clusters to photons:
 - Necessary to rebuild cluster
 - Necessary to re-calibrate cluster



Electron Identification Performance

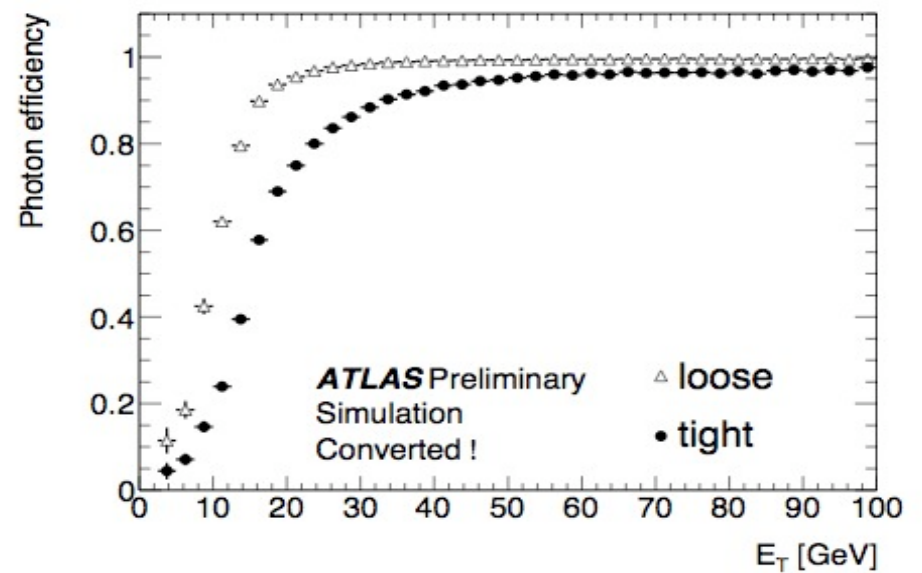
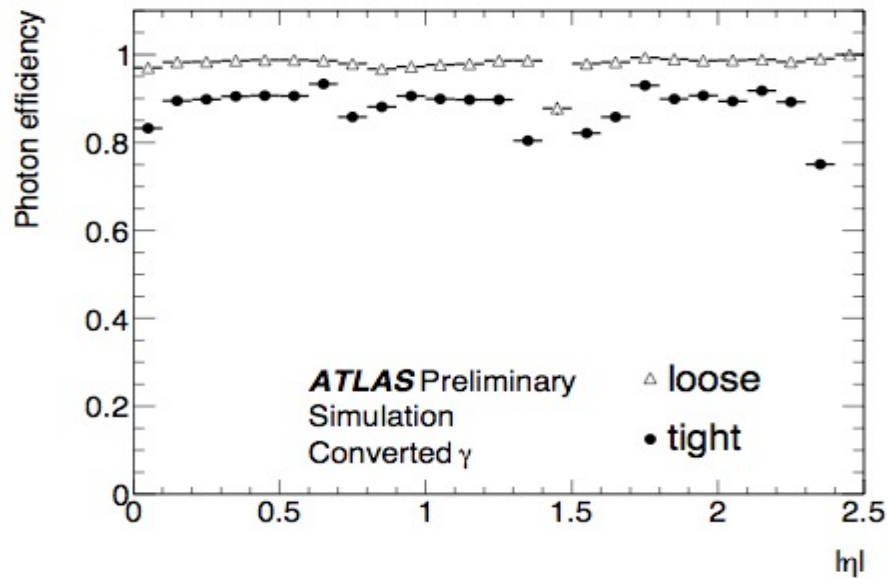
	Efficiency (%)		Jet Rejection (total)
	Z -> e e	b,c -> e	
Reconstructed	97.56±0.03	-	91.5±0.1
Loose	94.30±0.03	36.8±0.5	1066±4
Medium	89.97±0.03	31.5±0.5	6821±69
Tight	71.52±0.03	25.2±0.5	(1.38±0.06)×10 ⁵



Expected efficiencies for electrons with $E_T > 17$ GeV

Photon Identification Performance

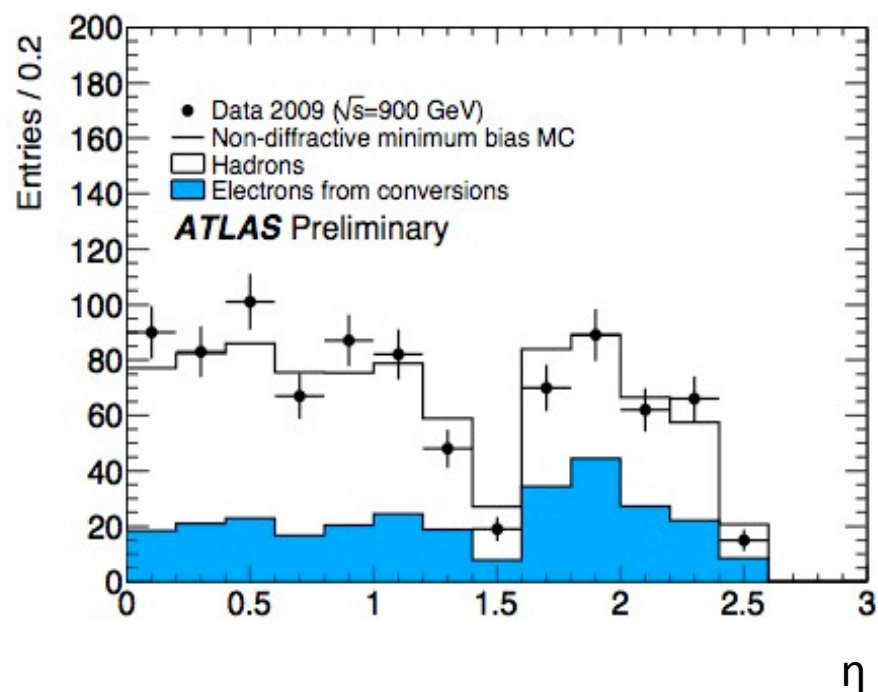
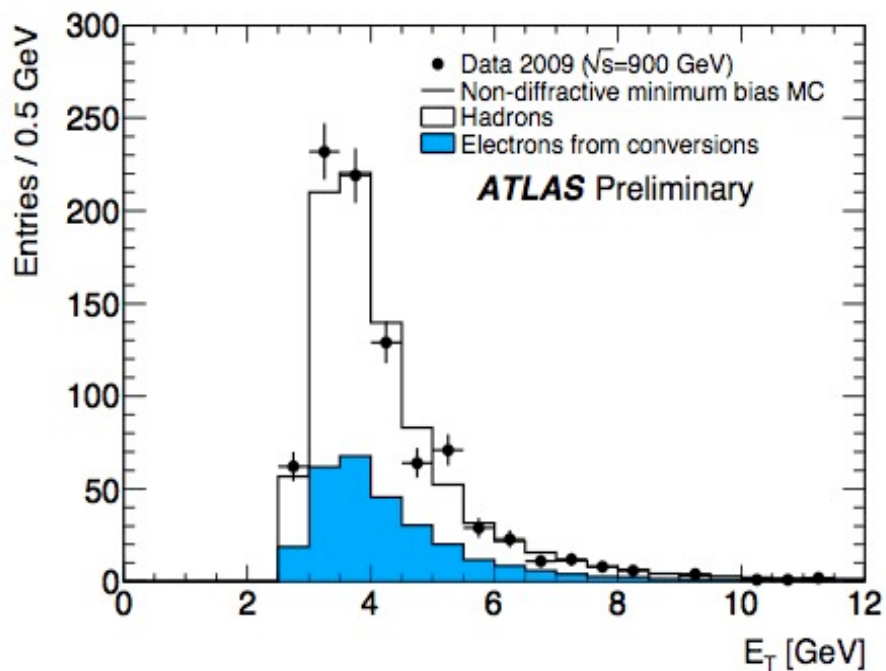
		$E_{\text{signal}}(\%)$	R
Loose	all	98.39 ± 0.01	908 ± 4
	unconverted	98.42 ± 0.01	
	converted	93.33 ± 0.01	
Tight	all	86.401 ± 0.02	4768 ± 43
	unconverted	84.90 ± 0.03	
	converted	89.27 ± 0.03	



Expected efficiencies for converted photons with $E_T > 20$ GeV

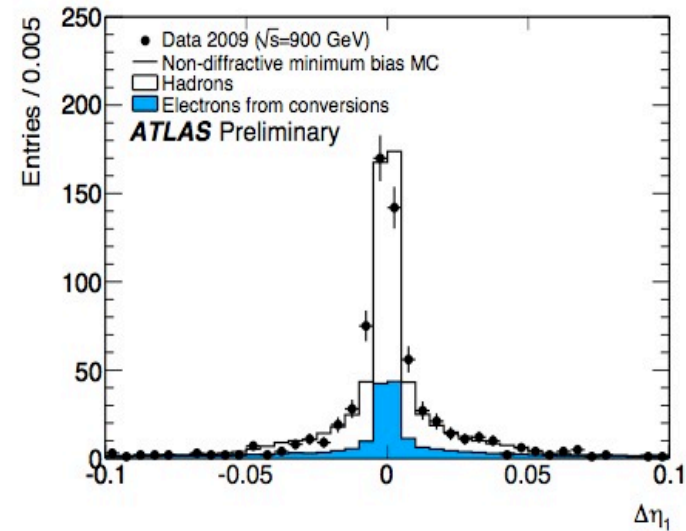
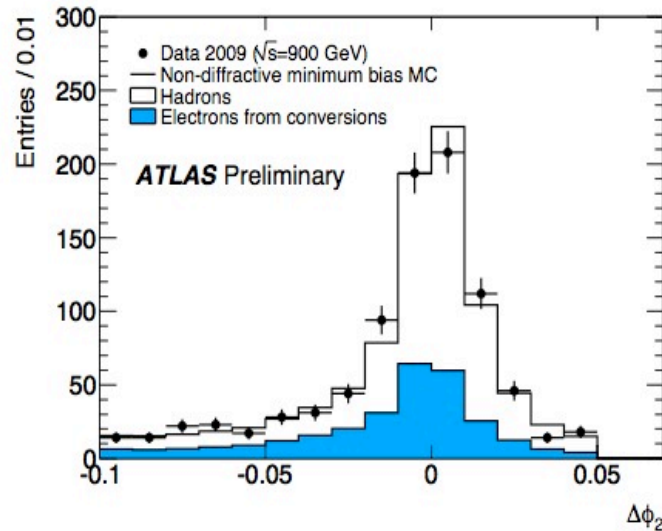
Electron Identification Performance: 900 GeV Data

Electron candidates	All		Barrel		Endcap	
	Data (%)	MC (%)	Data (%)	MC (%)	Data (%)	MC (%)
Loose	46.5±1.7	50.9±0.2	47.3±2.1	51.8±0.3	45.2±2.8	49.5±0.4
Medium	10.6±1.0	13.1±0.2	11.1±1.3	12.9±0.2	9.6±1.6	13.3±0.3
Tight	2.3±0.5	2.4±0.1	1.6±0.5	1.8±0.1	3.4±1.0	3.3±0.1

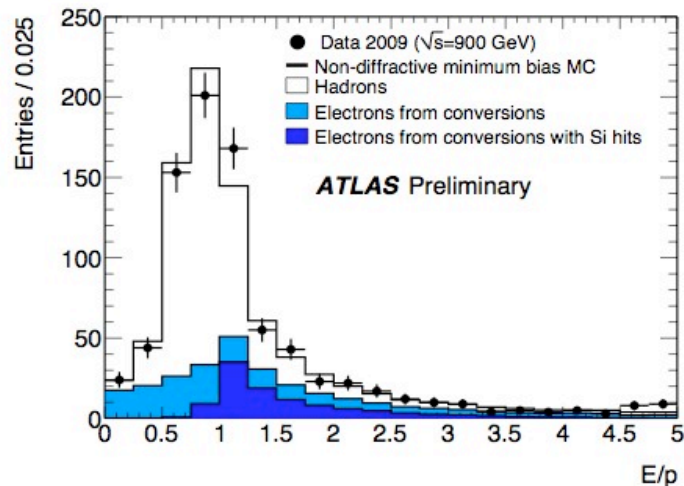


Track/Vertex-to-Cluster Matching: 900 GeV Data

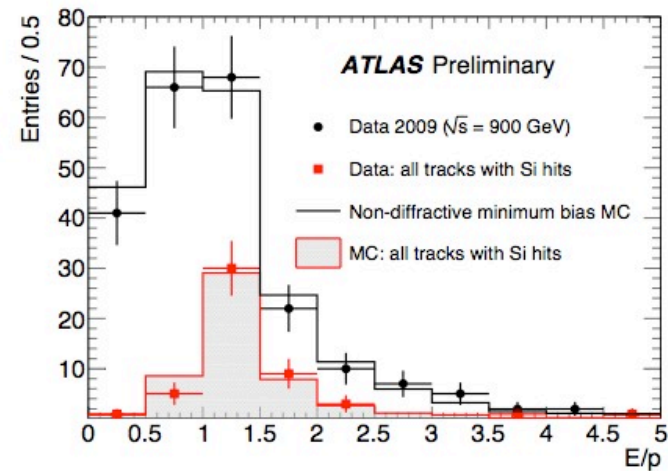
Track-to-cluster matching in η and ϕ . Successful matches determine an electron



E/p for electrons/converted photons. Tails towards small E/p due to poorly measured



Electrons



Converted Photons

Tracker Material Estimation using Converted Photons

Amount of material per tracker layer measured by estimating the fraction of converted photons

$$M = -9/7 \cdot \ln(1 - F_{\text{conv}}).$$

where

$$F_{\text{conv}} = \frac{N_{\text{rec}}^{\text{Data}} \cdot P^{\text{MC}} / A^{\text{MC}}}{N_{\text{all}\gamma}^{\text{Data}} \cdot \exp(-7/9 \cdot M_{\text{up}})}$$

$N_{\text{all}}^{\text{Data}}$ the number of incoming photons

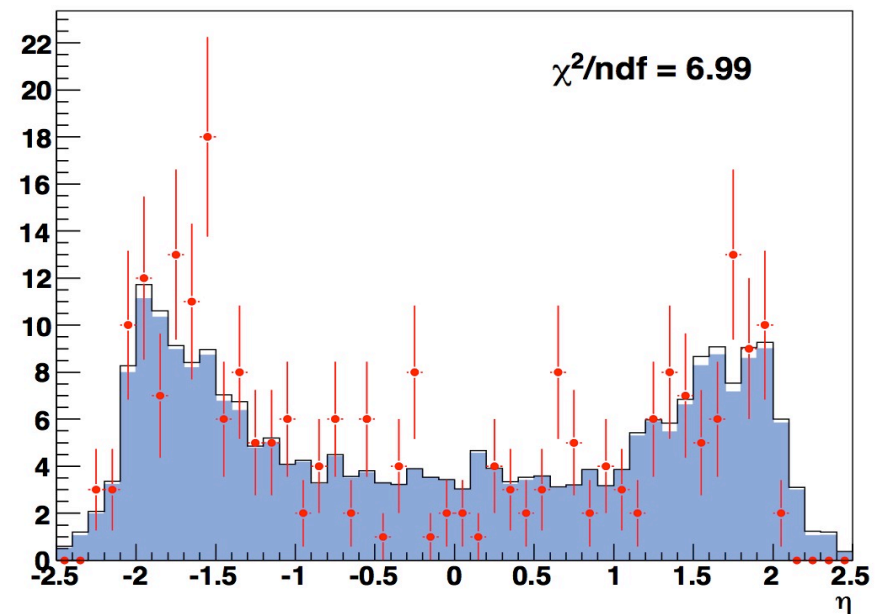
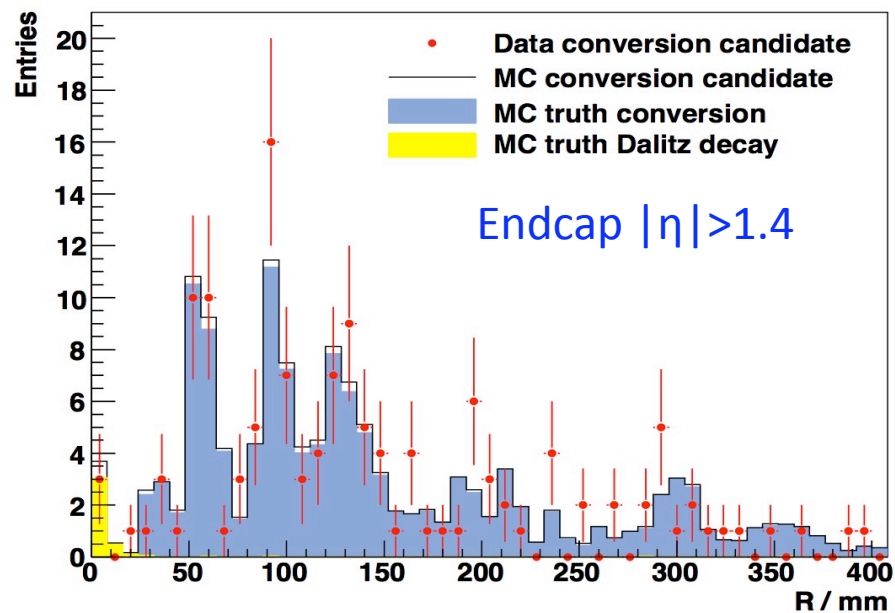
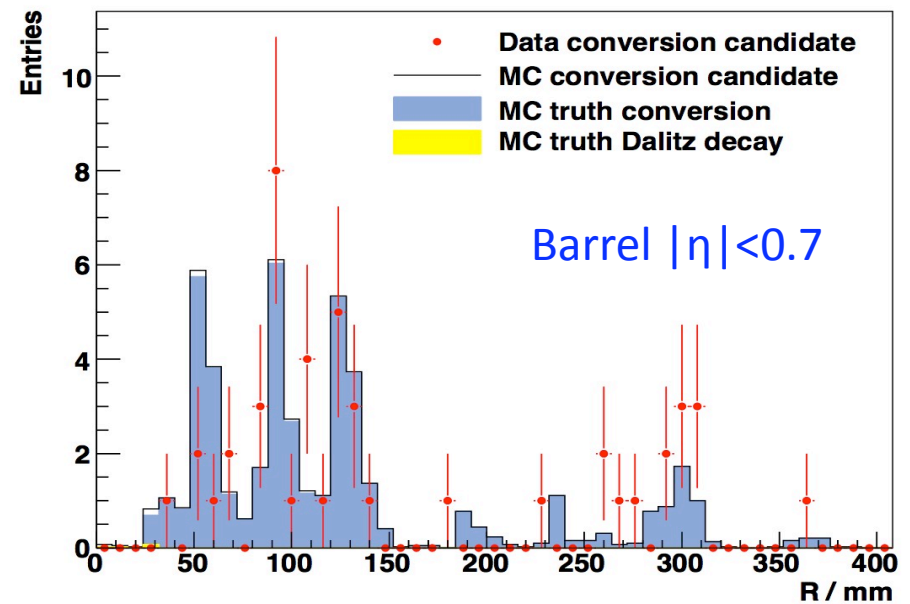
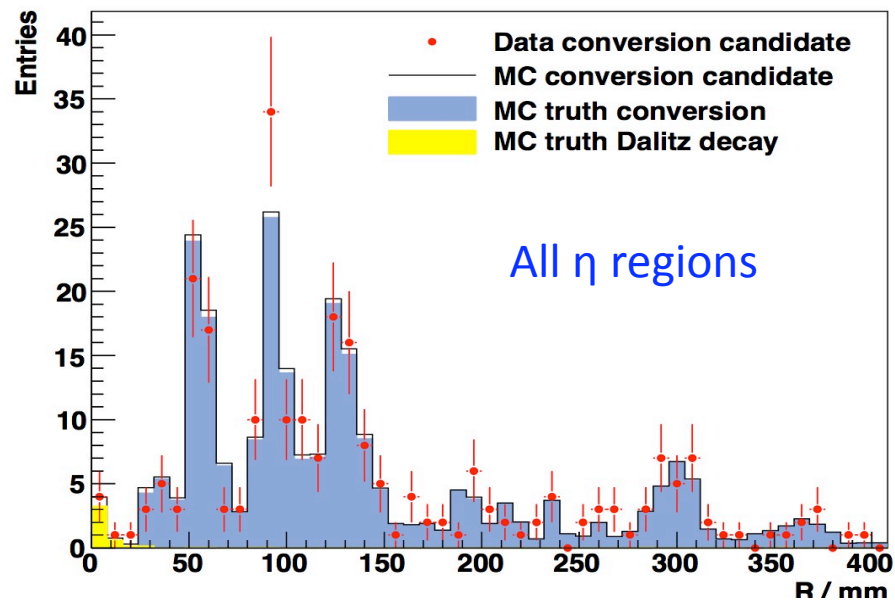
$N_{\text{rec}}^{\text{Data}}$ the number of reconstructed converted photons at the layer

M_{up} the upstream material

A^{MC} the selection efficiency

P^{MC} the fraction of correctly reconstructed conversion vertices at the layer

Reconstructed Converted Photons vs. Radius



Tracker Material Estimation using Converted Photons

Normalization to the beam pipe:

- Assume that beam pipe material correctly measured during construction ($X/X_0=0.0059$)
- Number of incoming photons inferred from the beam pipe material and the reconstructed number of converted photons
- Additional 30% uncertainty on normalization to the beam pipe material at current statistics

	Beam pipe	B-layer	Pixel 1	Pixel 2	SCT1
X/X_0 (data)	0.0059	0.0273	0.0367	0.0281	0.0236
Error X/X_0 (data)	0.0020	0.0041	0.0047	0.0039	0.0048
X/X_0 (MC)	0.0059	0.0290	0.0285	0.0260	0.0186
Error X/X_0 (MC)	0.0001	0.0002	0.0002	0.0002	0.0001
X/X_0 (Data/MC)	1.0000	0.9409	1.2902	1.0837	1.2645

Efficiency and Purities

	Beam pipe	B-layer	Pixel 1	Pixel 2	SCT1
Wrongly Reconstructed R	0.99	0.97	0.95	0.88	0.97
Efficiency	0.047	0.053	0.056	0.059	0.037
Combinatorial Background	0.91	0.97	0.98	0.97	0.99

Systematic Effects and Weaknesses

- Number of initial photons not well known ($N_{\text{all}\gamma}^{\text{Data}}$, for normalization)
 - ★ Entangled with overall reconstruction efficiency
 - ★ Currently: normalize to beam pipe (rather well-known radiation length)
 - ▶ 30% statistical uncertainty due to number of conversions on beam pipe
 - ★ Radiation length of beam pipe can be cross-checked with Dalitz decays

- Efficiency as a function of position
 - ★ Currently taken from Monte Carlo
 - ★ Can be cross-checked with efficiency for K_S in data and MC
 - ▶ Efficiency from K_S is optimistic: no bremsstrahlung, easier for vertex fit to converge due to non-zero opening angle
 - ★ Might be able to use Pixel Support Tube as point of reference

Need $O(10^9)$ conversions to understand all aspects (depends on (R,η) granularity

Summary and Conclusions

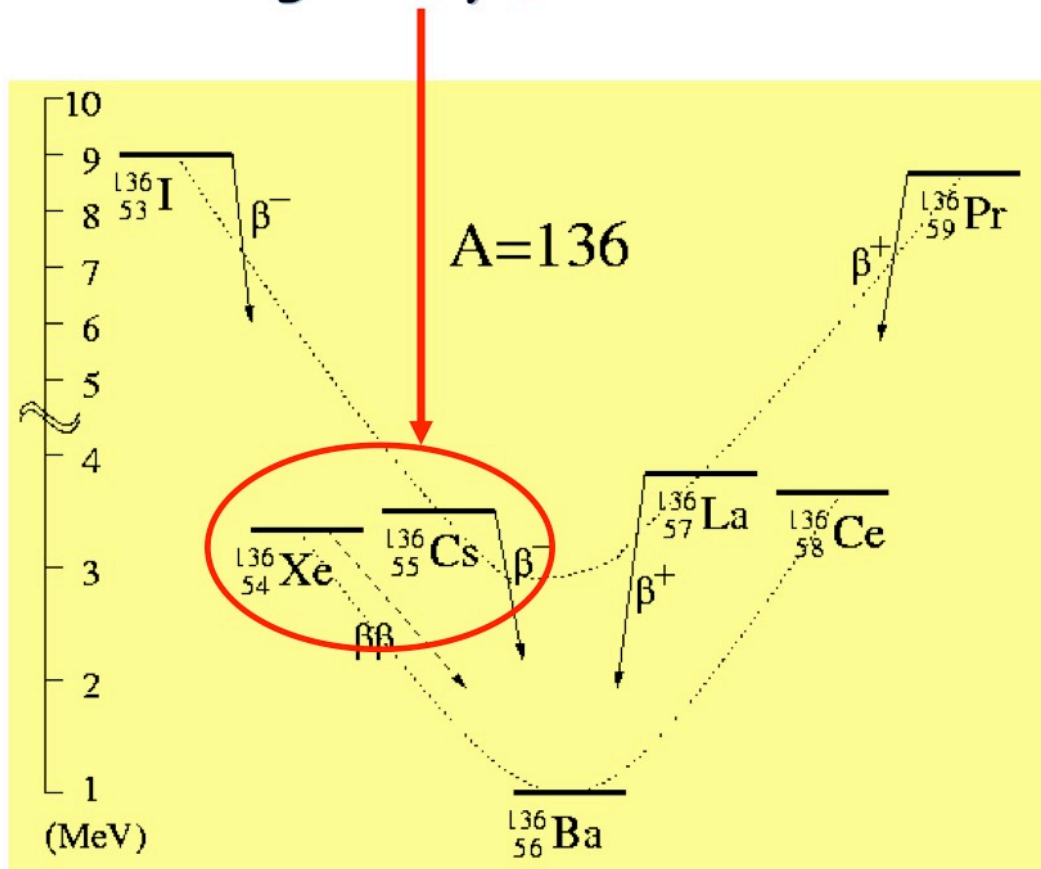
- Electrons constitute one of the most important objects for physics at the LHC
- An abundance of electrons will be produced already in the first year of the LHC running:
 - Thousands of high p_T ($>20\text{GeV}$) electrons from Z and W decays
 - Substantially more softer electrons from J/ Ψ decays
 - Countless soft electrons, primarily from converted photons, in minimum bias
- Electron reconstruction proceeds in two steps:
 - Track reconstruction including bremsstrahlung and other material interactions corrections
 - Combine with electromagnetic cluster to form the final electron object
- Paramount to resolve the ambiguities between electrons and converted photons
 - Large fraction of electrons originate from converted photons
 - The photon recovery procedure flags those electrons as converted photons
- Electrons have been reconstructed in the first 900 GeV LHC data
 - Calorimetric shower shapes and electron ID variables agree very well with predictions
 - Electron tracking also in good shape
 - The bremsstrahlung correction algorithms are being evaluated with data
- Converted photons have also been identified in abundance in minimum bias data
 - Electron tracking and conversion vertex reconstruction as expected from simulation
 - High purity conversions can be used for mapping the tracker material
 - Conversions provide a high purity electron sample for studying the TRT particle identification
- Overall electron and converted photon reconstruction in good shape with 900 GeV LHC data
- Looking forward for the upcoming 7 TeV runs to detect high p_T electrons from W,Z decays...

ENRICHED XENON OBSERVATORY (EXO)

Enriched Xenon Observatory: Double Beta Decay

Double-beta decay:

*a second-order process
only detectable if first
order beta decay is
energetically forbidden*



Candidate nuclei with $Q > 2$ MeV

Candidate	Q (MeV)	Abund. (%)
$^{48}\text{Ca} \rightarrow ^{48}\text{Ti}$	4.271	0.187
$^{76}\text{Ge} \rightarrow ^{76}\text{Se}$	2.040	7.8
$^{82}\text{Se} \rightarrow ^{82}\text{Kr}$	2.995	9.2
$^{96}\text{Zr} \rightarrow ^{96}\text{Mo}$	3.350	2.8
$^{100}\text{Mo} \rightarrow ^{100}\text{Ru}$	3.034	9.6
$^{110}\text{Pd} \rightarrow ^{110}\text{Cd}$	2.013	11.8
$^{116}\text{Cd} \rightarrow ^{116}\text{Sn}$	2.802	7.5
$^{124}\text{Sn} \rightarrow ^{124}\text{Te}$	2.228	5.64
$^{130}\text{Te} \rightarrow ^{130}\text{Xe}$	2.533	34.5
$^{136}\text{Xe} \rightarrow ^{136}\text{Ba}$	2.479	8.9
$^{150}\text{Nd} \rightarrow ^{150}\text{Sm}$	3.367	5.6

Enriched Xenon Observatory: Double Beta Decay

There are two varieties of $\beta\beta$ decay

2ν mode:
a conventional
 2^{nd} order process
in nuclear physics

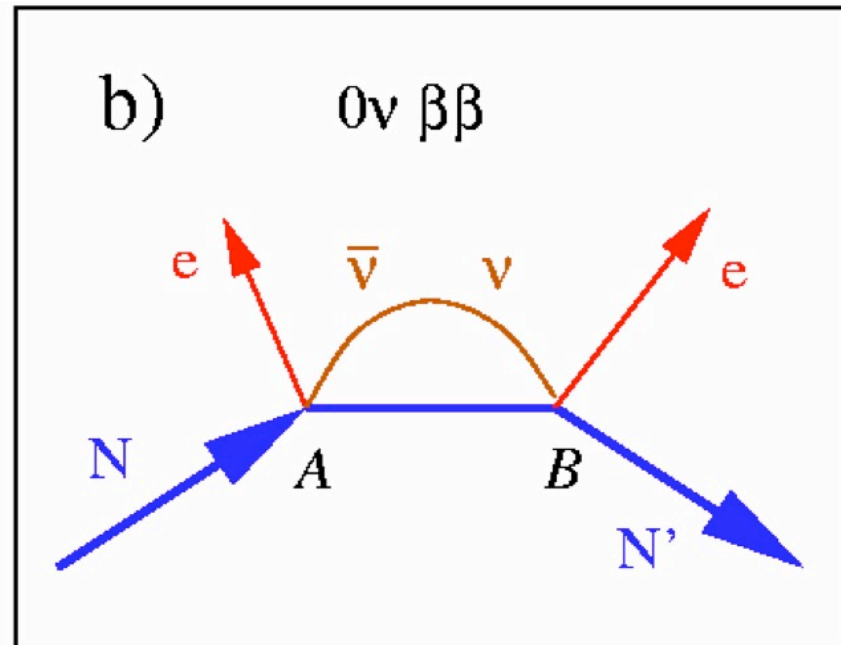
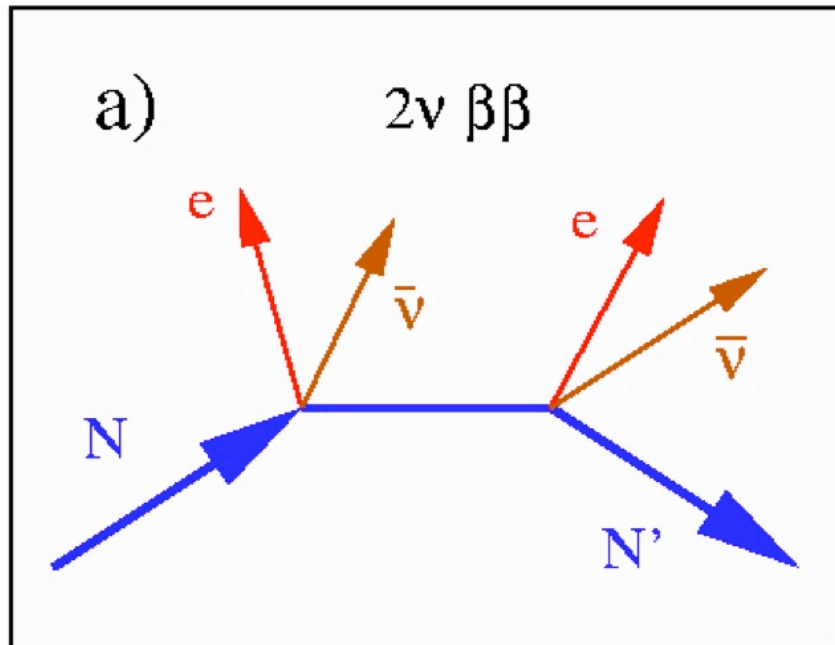
0ν mode: a hypothetical
process can happen

only if: $M_\nu \neq 0$
 $\nu = \bar{\nu}$ }

$$|\Delta L|=2$$

$$|\Delta(B-L)|=2$$

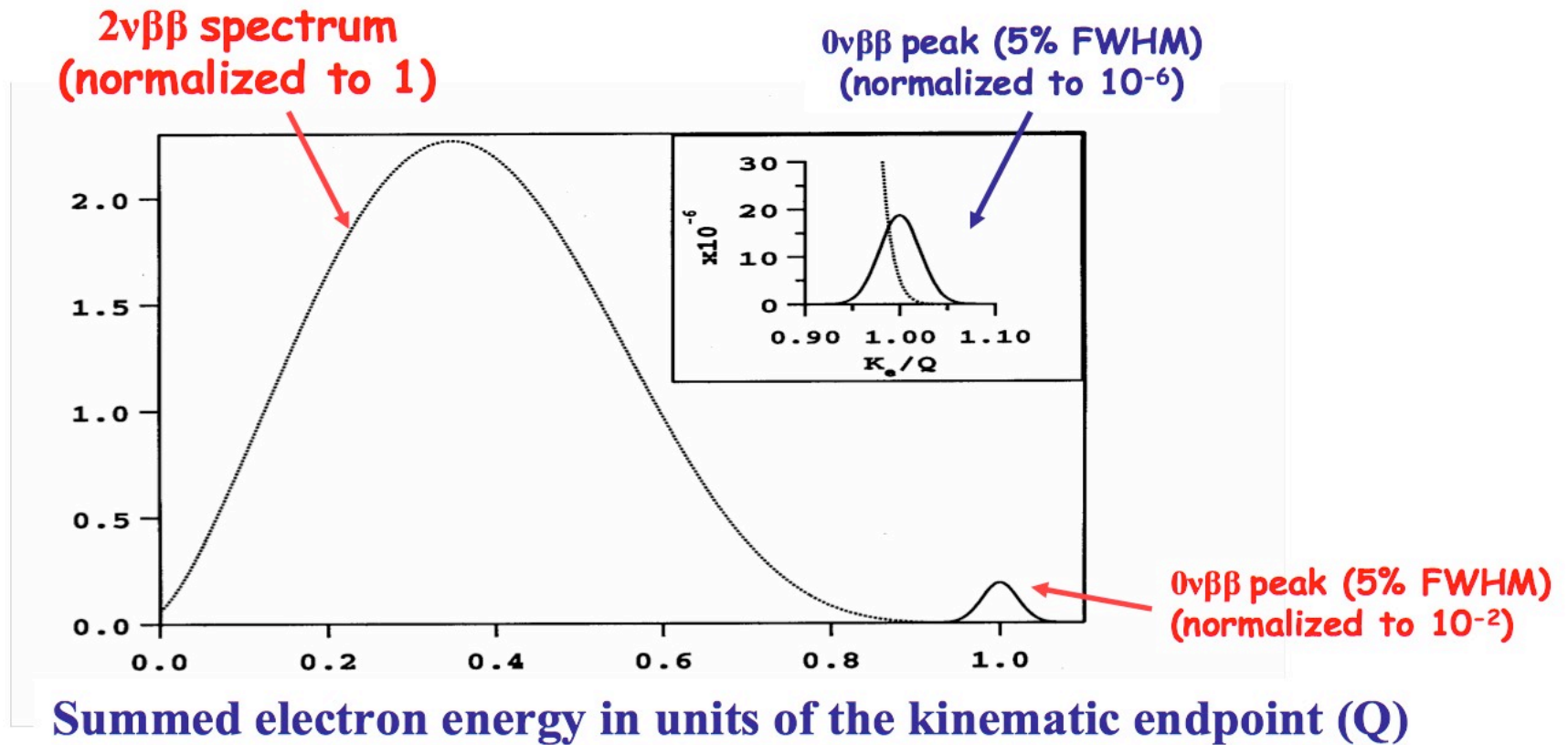
Since helicity
has to "flip"



Enriched Xenon Observatory: Double Beta Decay Spectrum

Background due to the Standard Model $2\nu\beta\beta$ decay

from S.R. Elliott and P. Vogel, Ann.Rev.Nucl.Part.Sci. 52 (2002) 115.



The two can be separated in a detector with good energy resolution

Enriched Xenon Observatory: Neutrino Mass

If $0\nu\beta\beta$ is due to light ν Majorana masses

$$\langle m_\nu \rangle^2 = \left(T_{1/2}^{0\nu\beta\beta} G^{0\nu\beta\beta}(E_0, Z) \left| M_{GT}^{0\nu\beta\beta} - \frac{g_V^2}{g_A^2} M_F^{0\nu\beta\beta} \right|^2 \right)^{-1}$$

$$M_F^{0\nu\beta\beta} \text{ and } M_{GT}^{0\nu\beta\beta}$$

can be calculated within
particular nuclear models

$$G^{0\nu\beta\beta}$$

a known phase space factor

$$T_{1/2}^{0\nu\beta\beta}$$

is the quantity to
be measured

$$\langle m_\nu \rangle = \sum_{i=1}^3 |U_{e,i}|^2 m_i \varepsilon_i$$

effective Majorana ν mass
($\varepsilon_i = \pm 1$ if CP is conserved)

Cancellations are possible...

Enriched Xenon Observatory: Neutrino Mass Measurement

To reach $\langle m_\nu \rangle \sim 10$ meV very large fiducial mass (tons)

(except for Te) need massive isotopic enrichment

Need to reduce and control backgrounds in qualitatively new ways

these are the lowest background experiment ever built

For no bkgnd $\langle m_\nu \rangle \propto 1 / \sqrt{T_{1/2}^{0\nu\beta\beta}} \propto 1 / \sqrt{Nt}$

Scaling with bkgd
goes like Nt $\langle m_\nu \rangle \propto 1 / \sqrt{T_{1/2}^{0\nu\beta\beta}} \propto 1 / (Nt)^{1/4}$

In addition a multi-parameter experiment, if feasible, would provide information for cross checks with more than one single variable, if a discovery is made.

Xe is ideal for a large experiment

- No need to grow crystals
- Can be re-purified during the experiment
- No long lived Xe isotopes to activate
- Can be easily transferred from one detector to another if new technologies become available
- Noble gas: easy(er) to purify
- ^{136}Xe enrichment easier and safer:
 - noble gas (no chemistry involved)
 - centrifuge feed rate in gram/s, all mass useful
 - centrifuge efficiency $\sim \Delta m$. For Xe 4.7 amu
- ^{129}Xe is a hyperpolarizable nucleus, under study for NMR tomography... a joint enrichment program ?

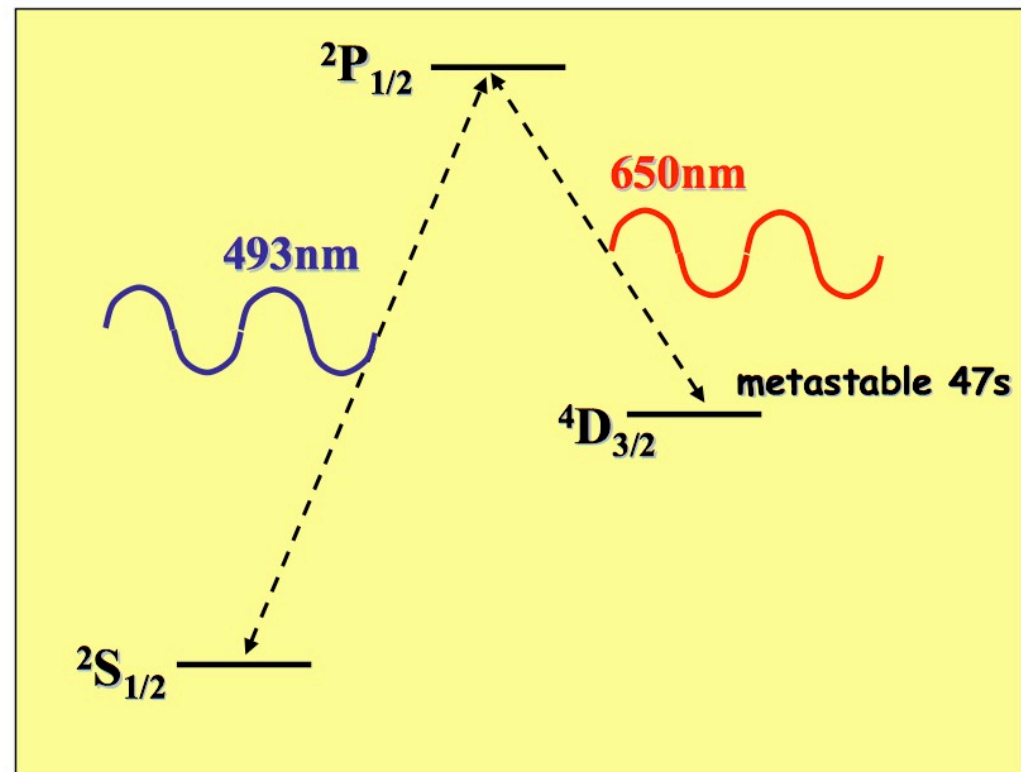
Enriched Xenon Observatory: Xe Spectroscopy

Xe offers a qualitatively new tool against background:
 $^{136}\text{Xe} \rightarrow ^{136}\text{Ba}^{++} e^- e^-$ final state can be identified
using optical spectroscopy (M.Moe PRC44 (1991) 931)

Ba⁺ system best studied
(Neuhauser, Hohenstatt,
Toshek, Dehmelt 1980)
Very specific signature
"shelving"

Single ions can be detected
from a photon rate of $10^7/\text{s}$

- Important additional constraint
- Drastic background reduction



Enriched Xenon Observatory: Mass Sensitivity

EXO-200kg Majorana mass sensitivity

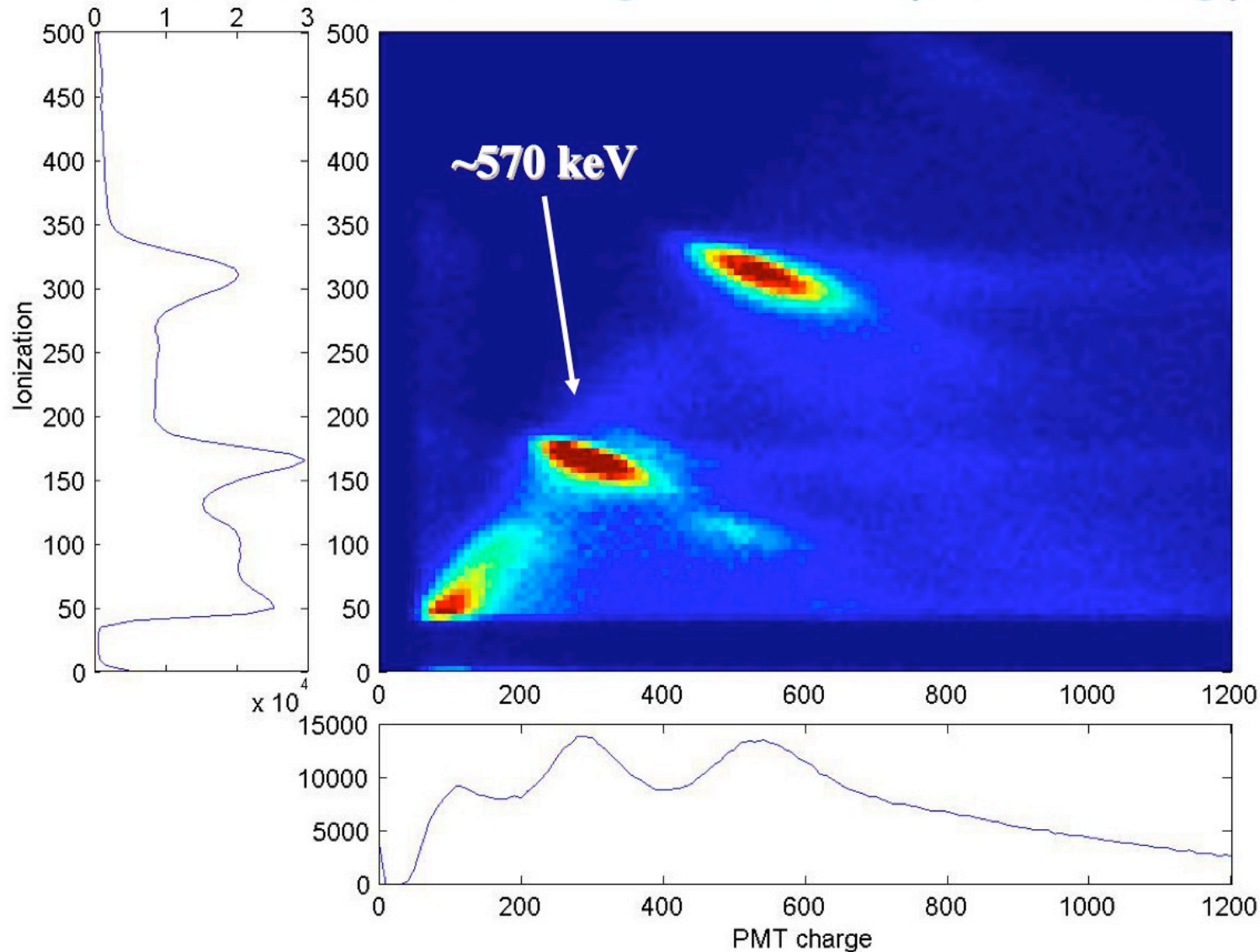
Assumptions:

- 1) 200kg of Xe enriched to 80% in 136
- 2) $\sigma(E)/E = 1.4\%$ obtained in EXO R&D, Conti et al Phys Rev B 68 (2003) 054201
- 3) Low but finite radioactive background:
20 events/year in the $\pm 2\sigma$ interval centered around the 2.481MeV endpoint
- 4) Negligible background from $2\nu\beta\beta$ ($T_{1/2} > 1 \cdot 10^{22}$ yr R.Bernabei et al. measurement)

Case	Mass (ton)	Eff. (%)	Run Time (yr)	σ_E/E @ 2.5MeV (%)	Radioactive Background (events)	$T_{1/2}^{0\nu}$ (yr, 90%CL)	Majorana mass (eV)	
							QRPA	NSM
EXO-200	0.2	70	2	1.6*	40	$6.4 \cdot 10^{25}$	0.133 [†]	0.186*
Conservative	1	70	5	1.6*	0.5 (use 1)	$2 \cdot 10^{27}$	24	33
Aggressive	10	70	10	1 [†]	0.7 (use 1)	$4.1 \cdot 10^{28}$	5.3	7.3

Enriched Xenon Observatory: Energy Resolution

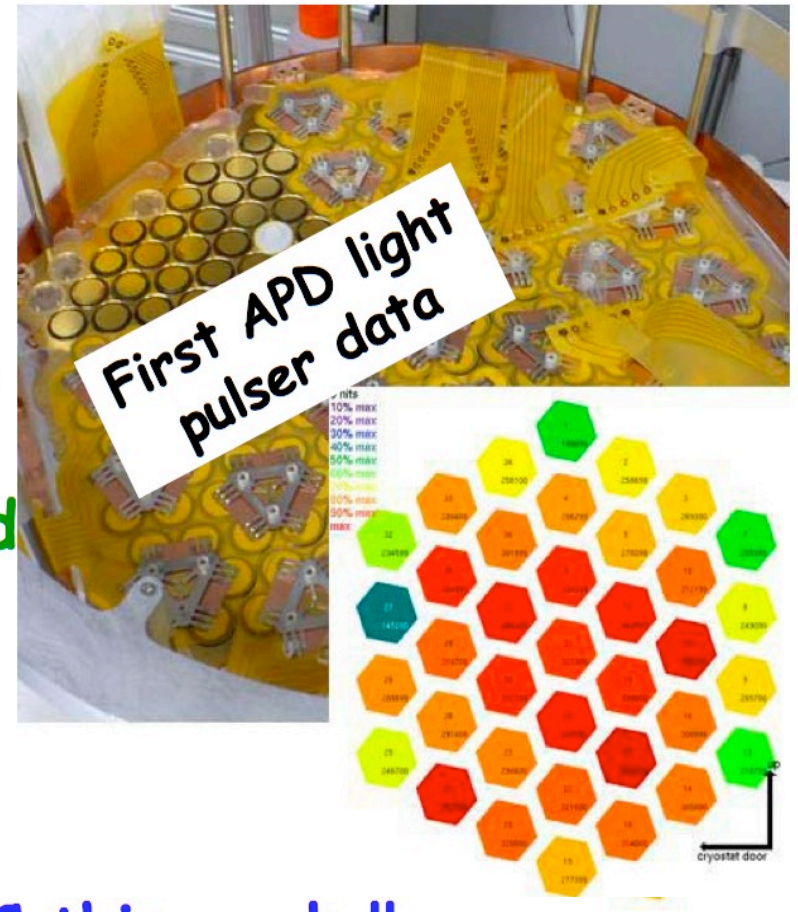
EXO R&D : *Use (anti)correlations between ionization and scintillation signals to improve energy resolution*



*E. Conti et al.
Phys. Rev. B68 (2003) 054201
and by now other groups have used this
[e.g. E. Aprile et al. PRB 76 (2007) 014115]*

Enriched Xenon Observatory: EXO-200 Summary

- TPC was tested with full electronics in the Summer 09 and passed all tests (but of course w/o LXe)
- TPC arrived WIPP on Nov 5, 09
- Everything but TPC commissioned at WIPP Nov-Dec 2009



- Install TPC this week !!
- Expect to start running sometimes before Summer 2010
- Xe purity issues always a concern

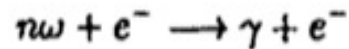
Pair production in Light-by-Light Scattering

Physics Motivation

- QED has been tested extensively in the weak field regime:
 - Perturbative methods are applicable and theory agrees extremely well with the experiment
- In the case of strong fields perturbative techniques are of limited applicability
 - Processes can be treated within a semi-classical theoretical frame
 - Theory not tested against experimental measurements
- Strong fields are defined with reference to the QED critical field strength

$$\mathcal{E}_{\text{crit}} = m^2/e = 1.32 \times 10^{16} \text{ V/cm} \quad (\hbar = c = 1)$$

- In fields of this strength various non-linear effects become prominent
- In this context the Breit-Wheeler process can be revisited
 - A multi-photon version of it could provide the necessary CM-energy to produce a e^+e^- pair
 - A two-step process in this approach using a laser induced external field:
 - A high energy electron scatters simultaneously off n laser photons, producing a high energy γ

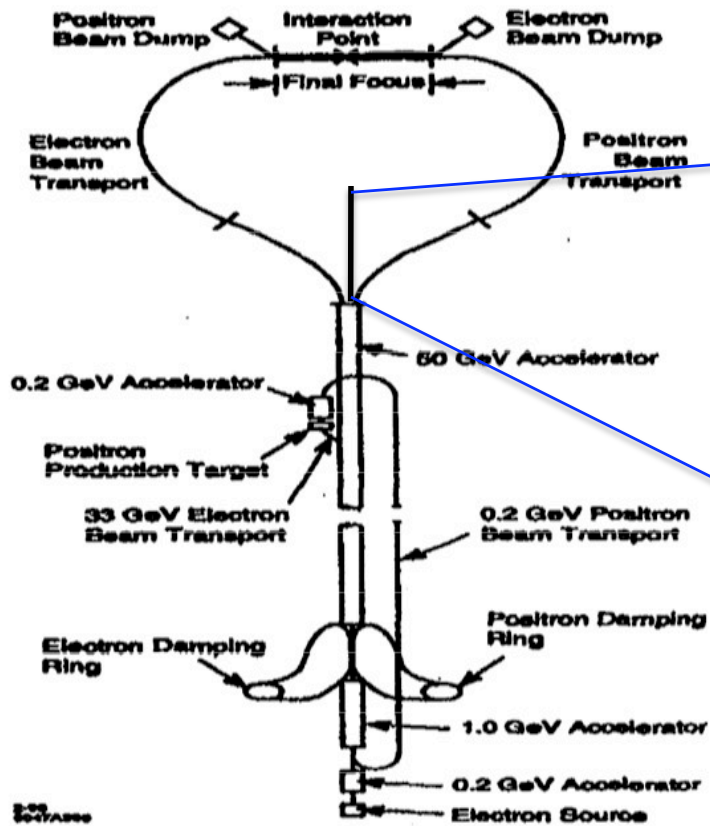


- The γ scatters again off n laser photons, while in the laser field, to produce a pair

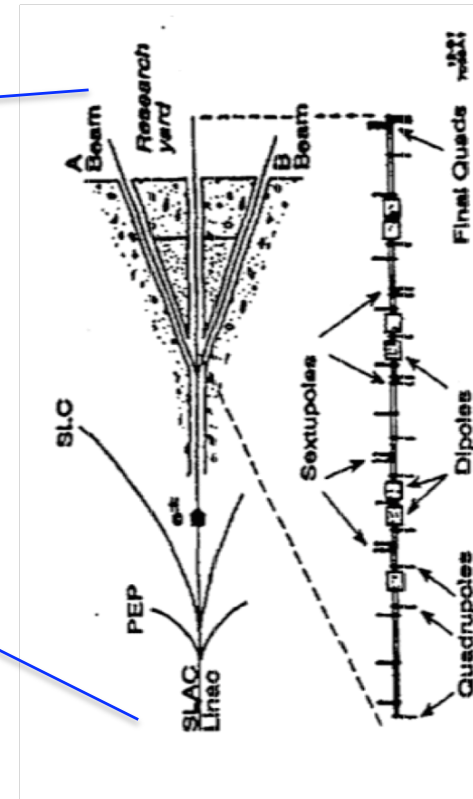


- This is the scheme employed by the E-144 experiment at SLAC
 - A table-top terawatt laser provided short pulses reaching a peak intensity of 10^{11} V/cm
 - At the rest frame of the 46.6 GeV electron beam it approaches the critical QED field strength
 - Pair production then becomes highly probable
- Results from this experimental effort will be presented here

The Electron Beam



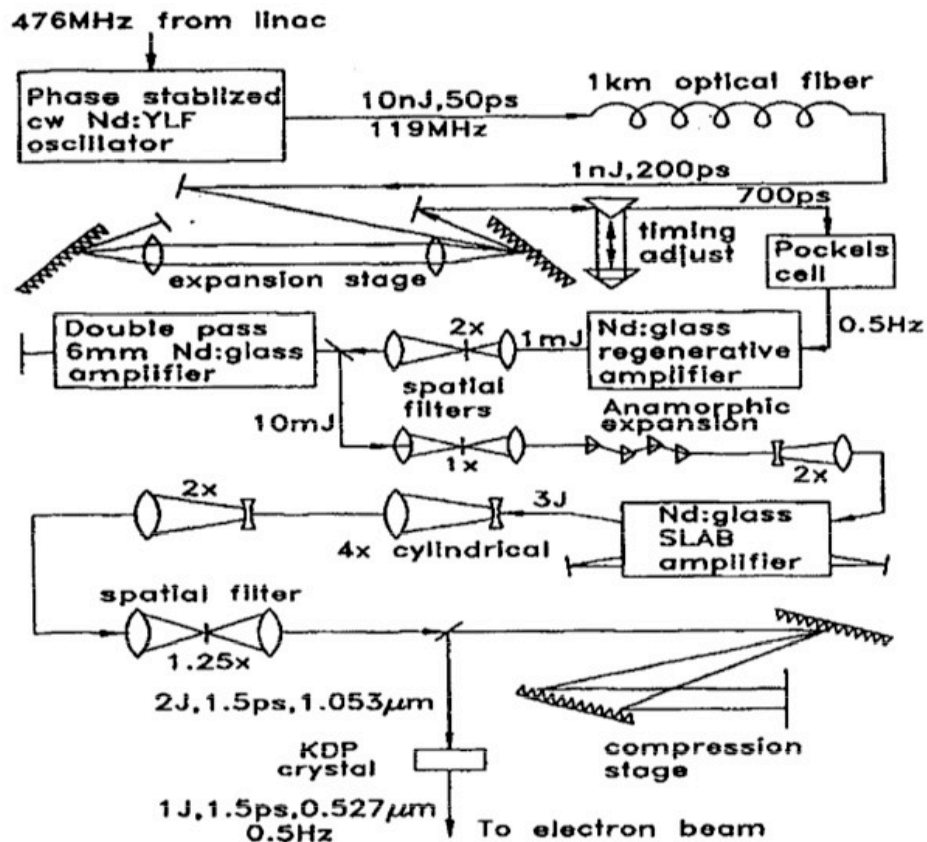
FFTB Line



- The experiment was installed in the FFTB line:
 - Located at the end of the 2-mile long linac
 - Line designed for focusing electron beams to sub- μm levels
 - No acceleration involved, pure beam optics line
 - Small focal areas increase the number of e^- through the laser beam and hence event rates
- Bunch lengths of <1 mm and beam charges of $5-7 \times 10^9$ have been delivered
- Normalized emittance of $3 \times 10^{-5}, 3 \times 10^{-6}$ in x,y transverse dimensions respectively
 - A measure of the electron beam size and divergence delivered at the FFTB line

Laser System

- The laser is a Table Top Terawatt (T^3) solid state system, that operates at 0.5 Hz
- Delivers both IR (1054 nm) and Green (527nm) pulse
- The polarization is chosen to be either linear or circular using a liquid crystal polarizer
- Maximum energies of 2J (for the IR) and 1J (for the green) have been delivered at the IP
- Focal points were 2 and 4.7 times the diffraction limited ones for the IR and green pulses.
- The pulse time widths are 1.5 ps for both wavelengths
- Intensities above 10^{18} W/cm² have been achieved at the focal point

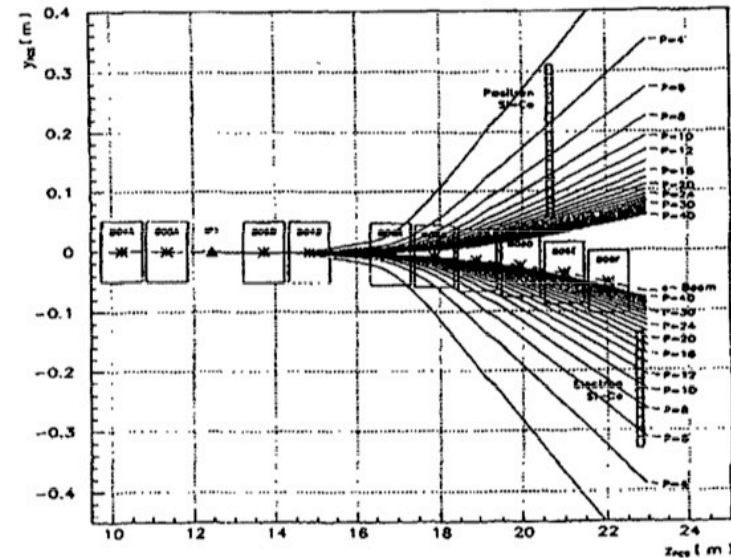
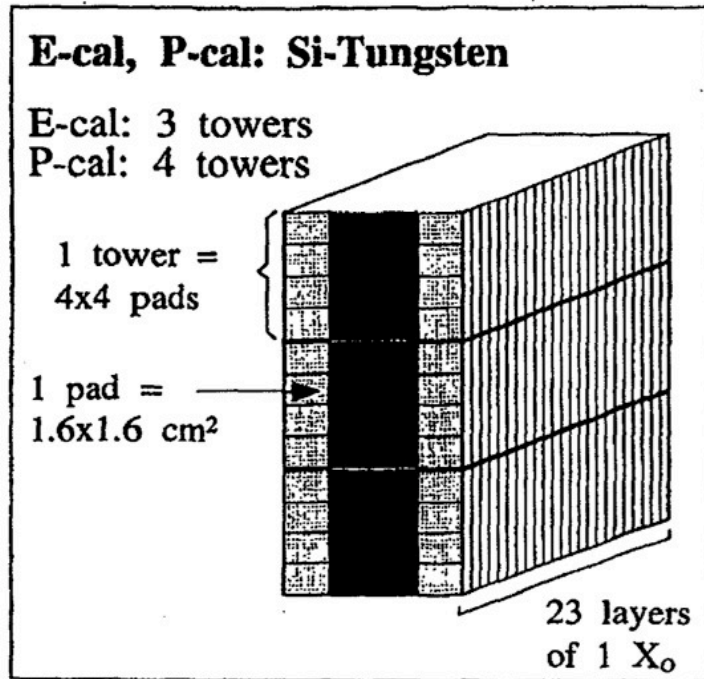


It consists of:

- An Nd:YLF modelocked oscillator
- An Nd:Glass regenerative amplifier (regen)
- A two-pass Nd:Glass rod amplifier
- A three-pass Nd:Glass slab amplifier

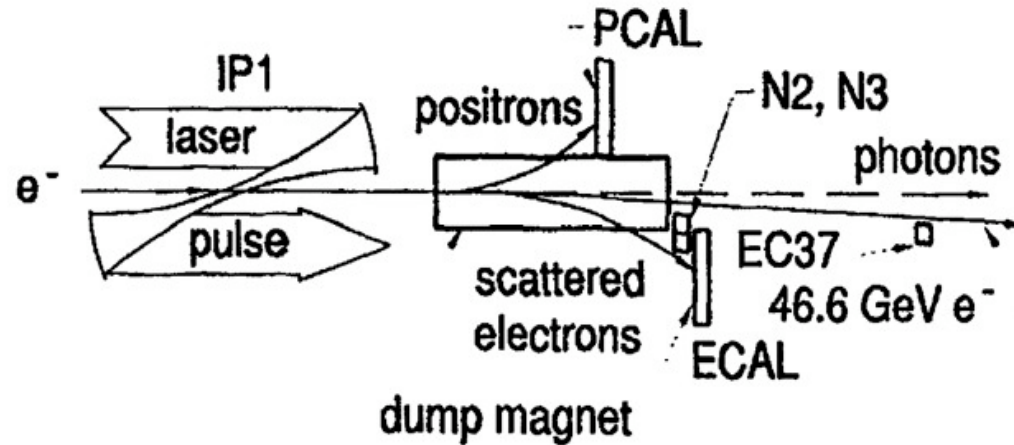
Calorimeters

- Two calorimeters are used to measure the energy of the charged particles, one for electrons (ECAL) and one for positrons (PCAL)
- Both calorimeters are of similar design



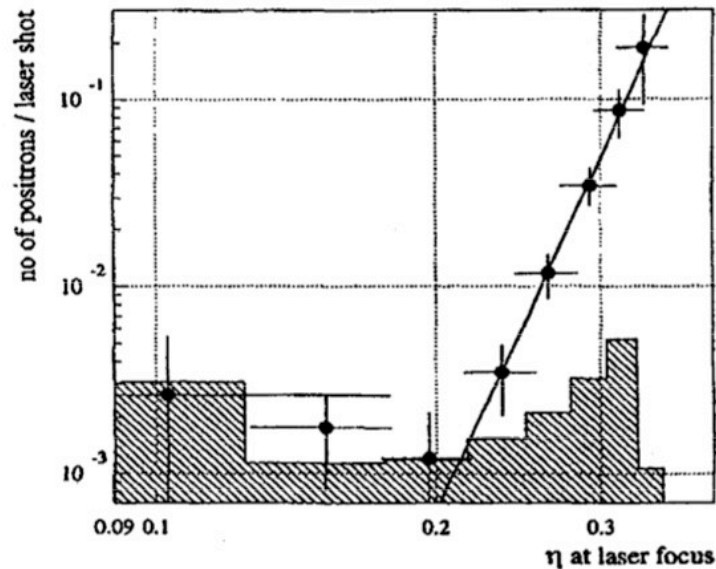
- Only the middle columns record signal, the outer columns used for background subtraction
- In addition linear/non-linear monitors
 - Linear monitors intercept electrons from linear Compton scattering
 - Non-linear monitors intercept electrons from 2nd/3rd order Compton scattering

Pair production in multiphoton light-by-light scattering 46.6 GeV electron beam data analysis



- A two-step process:
 - An energetic γ is produced by Compton scattering of 46.6 GeV e^- off n laser photons
 - While in the laser focus the γ absorbs $n(=4)$ laser photons to produce a pair
- Produced charged particles are deflected towards the calorimeters:
 - e^+ are deflected towards PCAL
 - Due to the rarity of the process all backgrounds need to be kept low in PCAL
 - e^- are deflected towards the ECAL
 - They are swamped by the Compton scattered electrons; signal impossible to extract
- PCAL the primary detector for the pair production
- Signal should be optimal when:
 - Laser intensity (described by η) highest
 - Laser-electron beam spatial/temporal overlap optimal

Multi-photon Pair Production Results

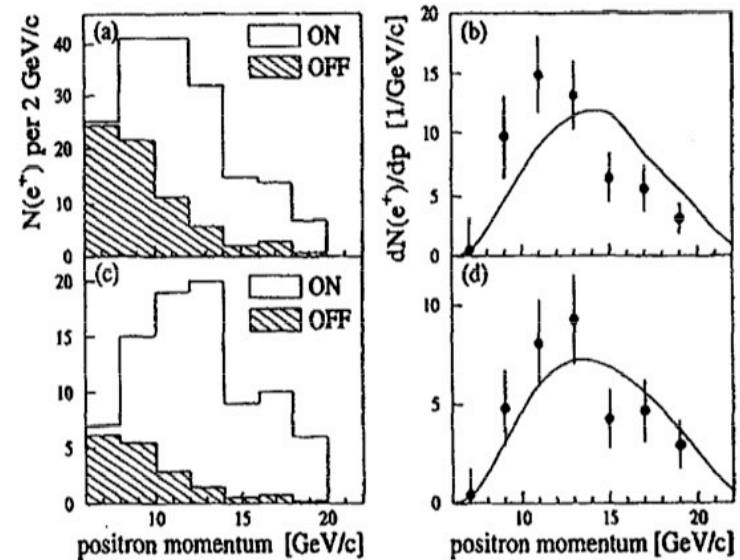


Total signal is 106 ± 14 positrons

Perform a power law fit. Slope indicative of the number of photons participating

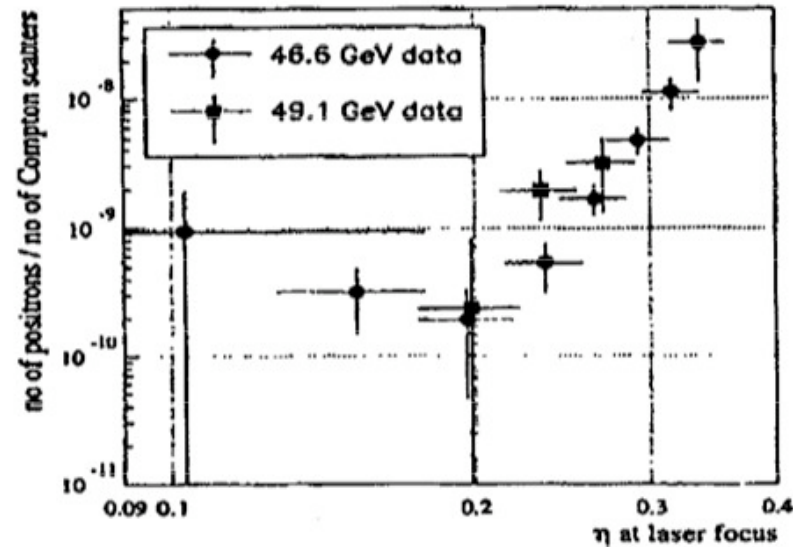
$$n = 5.1 \pm 0.2 \text{ (stat.) } \begin{matrix} +0.5 \\ -0.8 \end{matrix} \text{ (syst.)}$$

Low η region compatible with residual background from beam showering.
Concentrate on events with $\eta > 0.2$
Measured positron spectrum in good agreement with MC predictions.



Multi-photon Pair Production Results

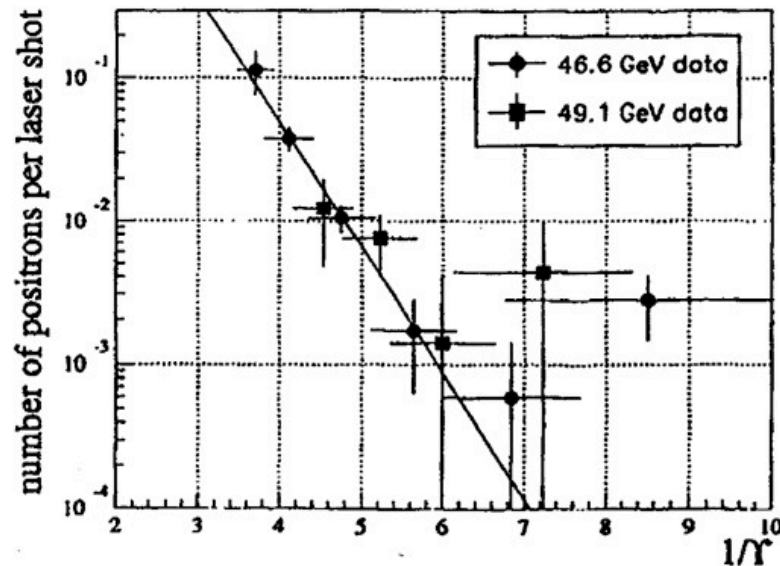
Another 22 ± 10 positrons have been accumulated at 49.1 GeV electron energy.



Putting them together with the 46.6 GeV data we see that the positron production rate increases by a factor of 2-3 as expected from the theoretical predictions

Spontaneous Vacuum Breakdown Results

- The pair production rates can be plotted as a function of $1/\gamma$
- In this case they should follow an exponential law
- This will be a manifestation of the spontaneous vacuum breakdown
- The dependence on $1/\gamma$ should be independent of the electron beam energy



Fitting an exponential one then obtains:

$$\pi g(1/\eta) = 1.78 \pm 0.11 \text{ (stat.) } \begin{matrix} +0.18 \\ -0.53 \end{matrix} \text{ (syst.)} \quad \text{Compare to 1.93 predicted by theory}$$

Summary and Conclusions

- The production of e^+e^- pairs during the scattering of an intense laser beam off a high energy electron beam has been observed experimentally
- The data can be successfully interpreted in two ways:
 - As a demonstration of the multi-photon Breit-Wheeler process within the regime of the non-linear QED
 - As the observation of “sparking” of the vacuum, within the context of vacuum polarization
- Semi-classical theoretical models describing non-linear QED effects have for the first time been tested experimentally. They were found to agree well with the measurements
- A new area of experimental research has been pioneered
 - Laser pulse-widths of ~ 1 ps have for the first time been produced and led to further improvements in the field of laser technology
 - Techniques developed for the timing of short beams have been widely employed since
 - The produced high energy γ 's with their small angular diversion (few μ -radians) have demonstrated a possible method for the production of a γ beam in future linear collider
 - A number of theoretical and experimental endeavors have sprung up since the conclusion of E-144
 - The field of strong-field and non-linear effects physics has been flourishing closely following the developments in laser technology
- The experiment itself and in particular the pair production results have received wide publicity over time. One can refer to the site www.slac.stanford.edu/exp/e144/popular.html